AD-787 660

ELECTROCALORIC REFRIGERATION FOR SUPERCONDUCTORS

National Bureau of Standards

Prepared for:

Advanced Research Projects Agency

30 June 1974

SEMI-ANNUAL TECHNICAL REPORT

ELECTROCALORIC REFRIGERATION FOR SUPERCONDUCTORS

ARPA Order 2535; NBS CC# 2750489

for the period ending June 30, 1974

Prepared by

Cryogenics Division
National Bureau of Standards, Institute for Basic Standards
Boulder, Colorado 80302

Sponsored by

Advanced Research Projects Agency
ARPA Order No. 2535

SUMMARY

of

SEMI-ANNUAL TECHNICAL REPORT

on

ELECTROCALORIC REFRIGERATION FOR SUPERCONDUCTORS

ARPA Order 2535; NBS CC# 2750489

for the period ending June 30, 1974

The goal of this program is to demonstrate the feasibility of a refrigerator based on the electrocaloric effect. It is planned to develop a prototype refrigerator which will absorb on the order of 1 watt at 4 K and have an upper reservoir temperature of 15 K. Applied research has been carried out mainly in two areas, (1) the glass-ceramic dielectric materials to be used as the refrigeration element and (2) heat switches to allow the cyclic refrigeration unit to be operated in a continuous manner.

The object of the dielectric studies has been to find the optimum manufacturing techniques for the $SrTiO_3$ glass-ceramics. The two important parameters of the glass-ceramics studied to date have been the temperature derivative of the dielectric constant, $\partial\epsilon/\partial T$, and the breakdown strength, E_B. These studies have revealed a problem with pitting in the manufactured samples which has limited the values of $\partial\epsilon/\partial T$ which can be reached to about 3 K^{-1}. The original design value was 25 K^{-1} and was based on earlier research samples. Possible solutions to the pitting problem have been under study. The values of E_B obtained to date are about 2.5 times the design value. An apparatus has been built to measure the field dependent specific heat, and the electrocaloric coefficient of the best samples obtained to date. The same apparatus will be used to look for a large cooling effect when large electric fields are applied.

Research on heat switches has been on both mechanical types and magneto-thermal types. The results obtained to date on a multiple leaf contact switch show that it can transfer the necessary 5 watts of heat with a ΔT of 1 K for use

as the upper switch. The switch ratios (defined as heat conducted in the "on" case to the heat conducted in the "off" case) may be as high as 270 but further work on such switch ratios is continuing. Preliminary results on the magneto-thermal conductivity of single crystal beryllium show that it can be used as a heat switch, with a field of 10-12 k0e required for the "off" condition. It promises to be a better switch than gallium.

A literature survey on the thermal conductance of joints (grease, adhesive, solder, pressure) indicate a serious lack of data in the range between 4 K and room temperature, especially in solder joints. Only rough estimates are possible at this time and these estimates on solder joints indicate design precautions must be taken to eliminate high thermal resistances at the joints. Because of its importance in the miniaturization of refrigerators, it is suggested that further research in boundary conductance be undertaken.

SEMI-ANNUAL TECHNICAL REPORT

on

ELECTROCALORIC REFRIGERATION FOR SUPERCONDUCTORS

ARPA Order 2535; NBS CC #2750489

For the period ending June 30, 1974

1. INTRODUCTION

The purpose of this project is to do research on manufacture-quality dielectric elements and on thermal valves leading to the goal of demonstrating the feasibility of a 1 watt electrocaloric refrigerator operating between 15 and 4 K. The overall concept of the device has been described previously.[1]

The main components of the electrocaloric refrigerator are the dielectric cooling element and the heat switches. The upper heat switch connects the cooling element to the 15 K reservoir whereas the lower switch connects the 4 K load to the cooling element. The research effort has been divided about equally between the dielectric materials and the heat switches. A small effort has also been spent on the problem of thermal conductances of joints. Joints will be inevitable when the various components of the refrigerator are put together in a working model.

The development of the dielectric materials ($SrTiO_3$ glass ceramics in this case) has been done primarily by Corning Glass Works personnel (W. N. Lawless and A. J. Morrow). The heat switch development and the thermal conductance of joints study has been done by National Bureau of Standards personnel (J. D. Siegwarth and R. Radebaugh).

2. DIELECTRIC MATERIALS

2.1. Dielectric Properties (A. J. Morrow and W. N. Lawless)

A few select compositions in the $SrO\text{-}TiO_2\text{-}Nb_2O_5\text{-}Al_2O_3\text{-}SiO_2$ system had been found previously at Corning Glass Works to display large $(\partial\epsilon/\partial T)_o$

values at low temperatures (2 to 20 K), to have nearly hysteretic-free P-E curves (up to 260 kV/cm), and to have very rapid phonon-polarization relaxation times.[1] Reported feasibility calculations were based on these materials.[1]

Previous experience at Corning Glass Works with these materials demonstrated that they could be fabricated into multilayer composites by an established capacitor-manufacturing process, and that the subsequent breakdown field strengths could exceed 10^3 volts per mil.[2]

Consequently, experimental multilayer samples for this program were fabricated in the development laboratory associated with the Corning Glass Works capacitor-manufacturing plant in Raleigh, NC. A total of four matrices of samples have been fabricated from these glass compositions to date, and sample size has been 3/4-in. square x 0.040 in thick. A fifth matrix is being fabricated, and each of these matrices consists of about 100 samples.

The thicknesses of the dielectric layers studied so far have been 0.001, 0.002, and 0.003 in., and the metal electrodes have been various combinations of Au, Pt, and Pd, applied by a silkscreen technique (approx. 0.0001 in. thick).

The purpose of these matrices has been to investigate the effects of various process variables on the low-temperature properties. It is important to bear in mind that these samples are about 10^3 larger than conventional glass-ceramic capacitors. The glass composition was maintained constant for each matrix, and the primary variables investigated included: dielectric thickness, metal electrode paste, heating rate, crystallization temperature, and hold time at temperature. The glass for these matrices was batched and melted at the Sullivan Park research facilities of Corning Glass Works in Corning, NY.

The capacitance and loss tangent of all samples were measured at 300 and 77 K in Raleigh, and favorable samples were shipped to Boulder for low-temperature measurements of ϵ vs. T, $(\partial\epsilon/\partial T)_o$, and E_B. A typical ϵ-T curve is shown in Fig. 1. Some measurements of $(\partial\epsilon/\partial T)_E$ and P(E) have also been made.

The primary properties are $(\delta\epsilon/\delta T)_o$ and E_B, and the previous research at Corning Glass Works showed that $(\delta\epsilon/\delta T)_o$ increases rapidly with crystallization temperature. This is shown in Fig. 2 by the curve labelled "FEP Research Samples" (note the logarithmic scale). The first two matrices studied both showed that $(\delta\epsilon/\delta T)_o$ increases even more rapidly with crystallization temperature between 1080 and 1100°C, but that slightly above 1100°C, $(\delta\epsilon/\delta T)_o$ deteriorated abruptly. The E_B properties behaved similarly. This is shown in Fig. 2 by the cross-hatched "band" labelled "FEP, FEL Multilayers."

Microscopic examination of these samples showed that a pitting or void-formation condition occurs just above 1100°C which is deleterious to both $(\delta\epsilon/\delta T)_o$ and E_B. This condition appears endemic to the large sample size and was therefore unforeseen. The behavior of $(\delta\ell n\epsilon/\delta T)_o$ through this pitting temperature range is smooth and monotonic and suggests that the glass-ceramic material is behaving properly aside from the voids.

The glass-ceramic efforts next split into two areas: (1) attempts to solve the pitting condition, and (2) further matrix studies to determine optimum process conditions up to 1100°C.

2.1.1. Attempts to Solve Pitting. The work here involved process approaches in the Raleigh plant and supplementary work at the Sullivan Park research facilities.

The first efforts were diagnostic in nature to determine the source of gas in the samples. Several pitted samples were ruptured in a mass spectrograph and CO_2 was detected. There are three possible sources of CO_2: The glasses are batched with carbonate powders; there is an organic binder in the glass frit; and an organic binder in the metal electrode paste.

A glass was batched and melted which contained no carbonate batch powders, and some samples of this glass were fabricated without metal electrodes and crystallized above 1100°C. These samples were as pitted as the original samples, so the CO_2 source was narrowed to the organic binder in the glass frit.

A number of approaches were taken to attack the organic-binder CO_2 source, and several of these studies are still in process. An alternate manufacturing process using what was believed to be a possibly more favorable binder was tried, but this also resulted in pitted samples, shown by the data labelled "FHJ-Warden" in Fig. 2. Attempts were made to crystallize the samples under very high viscosity conditions, the idea being to see if a very "stiff" glass matrix would contain void expansion. These results, labelled "FHJ-AVC" in Fig. 2 were also disappointing. This approach is still being pursued to see if various viscosity levels will ameliorate the pitting.

Another approach tried was to crystallize samples in a vacuum at slow heating rates to facilitate the CO_2 evolution. Samples so processed were extensively damaged by too rapid gas evolution.

One promising approach nearly completed is to simply eliminate all organic binders by processing glass sheets interleafed with Pt foil. If successful, this method would not, however, easily lend itself to an existing manufacturing process but rather would entail hand stacking.

An approach being pursued in Raleigh on a somewhat long-term basis is to systematically study the effects of glass-frit particle size, cast viscosity, binder burnout procedure, etc. on the pitting problem.

It was known from x-ray diffraction measurements that a small amount of a strontium feldspar phase crystallizes at about 1100°C in these particular alumino-silicate glass systems. It was suggested that this secondary phase crystallization may be nucleating the CO_2 evolution. This feldspar crystallization is inhibited in boro-alumino-silicate systems, so long-range glass composition studies were initiated in these systems. The results obtained on research samples of the first glass-ceramic studied are shown in Fig. 2 in the curve labelled "Boro-alumino-silicate (FHK)". Additional systems' studies here are aimed at improving $(\partial\epsilon/\partial T)_o$, because x-ray data do show the absence of the feldspar phase.

2.1.2. Optimum Process Variables below 1100°C. In parallel with the work mentioned in 2.1.1 above, additional matrix studies were made to determine the best process variables prior to the onset of pitting.

These matrix studies build one on another in that the results of a particular matrix are applied to the next matrix, etc. The three matrices characterized so far have clearly delineated the best process variables below 1100°C -- metal electrode paste, glass composition, dielectric thickness, heating rate, hold time, etc.

The relation between dielectric thickness and breakdown strength E_B has been very encouraging, and these data are shown in Fig. 3. There is a distinct trend in E_B increasing with dielectric thickness. This is very favorable because the thicker the dielectric layers, the less metal in the electrodes, and hence the smaller the thermal loading. Another advantage here is that smaller element capacitances lead to shorter charging times.

This improvement in E_B with thicker dielectric layers is probably due to the very small probability of "in-line" defects with the thicker layers (the layers are built up with .001-in layers). This trend is being studied further with .004 to .006-in. dielectric layers.

Another feature evident in Fig. 3 is that the E_B values obtained with the .003-in. dielectric layers are about 2-1/2 to 3 times larger than the design strength for a 1 watt refrigerator.[1] Therefore, some trade-off is possible between the larger E_B values but smaller $(\partial\epsilon/\partial T)_o$ values obtained in these samples.

2.1.3. Future Plans. Future plans for the dielectric materials will involve three parallel efforts: (1) to measure the electrocaloric coefficient and specific heat on the "best" samples made to date at 1100°C (note that the former measurements would demonstrate cooling, see below); (2) to continue refining the optimum process conditions up to 1100°C; and (3) to continue with approaches to solve the pitting problem.

2.2. Electrocaloric Properties Measurements (W. N. Lawless)

The state function for dielectrics is $(\partial P/\partial T)_E$, where P, E are polarization and electric field, respectively, and an experimental determination of this state function would allow design studies to be carried out for any type of solid-state refrigeration cycle (analogous to knowing pressure-volume-temperature data for a gas). Moreover, knowing $(\partial P/\partial T)_E$ would provide a basis for both building a prototype and judging test results.

Thermodynamically, the state function is given directly by

$$(\partial P/\partial T)_E = -C_E \beta_E / T,$$

where C_E is the field-dependent specific heat and $\beta_E = (\partial T/\partial E)_S$, the electrocaloric coefficient.

Techniques and the associated computer processing have been developed to measure C_E and β_E in the temperature range 2-20 K on dielectric materials in general and on the glass-ceramic samples from Raleigh in particular. The same experimental apparatus can be used for both measurements.

The experimental methods were complicated by a number of considerations: (1) Because of the large voltages involved, it did not seem advisable to use any heat switches to cool or isolate the sample (i.e., no moving parts); (2) Because of the relatively small specific heat of glassy materials and also because the specific heats of some addenda are not accurately known above 4 K, it was necessary to maintain the addenda to the smallest amounts possible; (3) Sample thermometry was limited to tiny carbon resistors whose accuracy/repeatability in the range 2-20 K required investigation.

A pulse-type technique was adopted where the sample is rigidly mounted to the reservoir (in this case, a temperature-controlled copper can enclosing the sample) through a thermal link (see inset in Fig. 4). It was desirable to have one thermal link span the entire 2-20 K range, and this proved troublesome.

The time constant τ of the link varies as $C/\mathcal{K}$, where C is the heat capacity of the sample, and $\mathcal{K}$ is the thermal conductance of the link. For a metal link, $\mathcal{K} \propto T$, whereas $C \propto T^3$ for insulators, so that $\tau \propto T^2$ -- i.e., a favorable τ at 2 K (say, 30 sec) would lead to an unacceptably long τ at 20 K ($\sim$ 1500 sec). Moreover, such a metal link would mean very long cool-downs.

Graphite is known to have $\mathcal{K} \propto T^{2.5}$, so carbon resistors were experimentally studied for use as thermal links. Here the competing factors are favorable τ's, 2-20 K, vs. thermal loading as an addendum. Data measured on Allen-Bradley radio resistors with Raleigh samples are shown in Fig. 4, where for comparison a metal link is also shown. The 2.7 Ω - 1/2 W resistor was selected because this resistor not only yields favorable τ's, 2-20 K, but also is not heavy ($\sim$130 mg with the phenolic resin machined off and leads trimmed to $\sim$3mm).

The experimental concept here is that following a heat pulse (C_E case) or voltage change (β_E case), the sample temperature first changes rapidly then decays back to the reservoir temperature through the thermal link. Analysis of the decay data yields ΔT, the temperature change.

One end of the thermal link is simply indium-soldered into the reservoir. The other end attaches to the sample, and it was found that the glass-ceramics could satisfactorily be attached by first firing a thin layer of glass-fritted silver to the ceramic, followed by indium-soldering the link to the silvered region. The indium joint was trimmed to minimize the addendum.

A sample for this method consists of two Raleigh samples bonded together sandwich-style with a heater in between. The bonding agent is G. E. 7031 varnish, and it is critical to use only the smallest amount of this varnish for two reasons: (1) The specific heat of 7031 is relatively huge, $\sim$30 times as large as copper; and (2) The specific heat depends on certain imponderables such as varnish dilution, drying time, etc. This problem was solved by first

wrapping the heater wire in a specific pattern on a special jig, transferring the heater from the jig to one of the samples with narrow strips of tape, applying a fine coat of 7031 to the heater wires, and finally removing the tape after the 7031 had dried. The second Raleigh sample was then bonded using a few small droplets of 7031.

The importance of maintaining the Indium and G. E. 7031 to the barest possible amounts for these glass-ceramics was learned the hard way: In four preliminary runs, it was later discovered that the In + 7031 constituted ~70% of the total heat capacity.

A schematic drawing of an assembled and attached sample is shown in Fig. 5. Typical sample and addenda weights are: sample, ~3g; G. E. 7031, ~10 mg; In solder, ~20 mg; graphite, ~30mg; copper, ~10 mg -- addenda weights ~2-3%.

The above sample weight includes the metal electrodes, and this particular addendum presents a dilema: Although for thick dielectric layers the amount of metal is relatively small, the specific heat contribution can be significant (Au, Pt, Pd), and there is no precise gravimetric method for determing the metal content in a particular manufactured sample. We have decided to use the specific heat measurement itself to determine the metal content by a difference method: The plant in Raleigh has prepared samples without electrodes, and by accurately measuring the specific heat of an unelectroded sample and its companion electroded sample, the metal content can be precisely determined.

Allen-Bradley 220 Ω - 1/8 W resistors were selected for sample thermometers because of their small size and favorable thermometric properties in the range 2-20 K. In any one run, these resistors were selected for sample thermometers because of their small size and favorable thermometric properties in the range 2-20 K. In any one run, these resistors accurately follow the empirical equation

$$\log R = A + BT^{-P};$$

e.g., correlation > 0.9999. Studies of these resistors showed, however, that on subsequent runs the coefficients A, B, and P changed sufficiently to introduce significant errors in ΔT, the quantity of interest (note that $\Delta T/T \sim 3\%$).

This problem was solved as follows: First, a silicon diode on the reservoir was calibrated against a Ge thermometer and the repeatability of this diode was good enough (<0.5 mK, three runs) to adopt it as the standard temperature reference (this diode also acts as the control thermometer for a commercial temperature controller). The sample and reservoir must be in equilibrium before the heat pulse or voltage change, and from these equilibrium points taken throughout the run, the resistor is calibrated against the diode according to the above equation. Only B and P are retained from this overall fit; the coefficient A is repeatedly determined at each equilibrium point. In this fashion, the resistor is made to match the diode exactly at the equilibrium point, and the subsequent ΔT reflects the excellence of the overall fit.

All the experimental and computational bugs are now worked out of the method, and sample measurements are underway.

2.2.1. Thermal Conductivity Measurements. Knowledge of the thermal conductivity of these glass-ceramics will be needed for eventual prototype design, so a method for measuring thermal conductivity in the range 2-20 K was established in parallel with the above specific heat-electrocaloric coefficient method. The two methods involve much of the same equipment and thermometry handling, but the thermal conductivity measurement is by far the simpler experiment.

In Fig. 6 are shown thermal conductivity data measured on three glass-ceramics (Code 9658, FEO, FEP) and on fused silica. The fused silica data agree very well with published data, and the amount of glass phase present decreases from FEP to FEO to Code 9658.

3. HEAT SWITCHES

The electrocaloric refrigerator, like the adiabatic demagnetization refrigerator[4], requires two thermal valves or switches, one to transfer heat from the refrigeration material to the high temperature heat sink and the other to transfer heat from the cooled region to the refrigeration material. The superconducting heat switches used for the demagnetization refrigerator cannot be used on this electrocaloric refrigerator because of the higher operating temperatures. Suitable heat switches for the electrocaloric refrigerator require considerable development.

3.1. Mechanical switches (J. D. Siegwarth and R. Radebaugh)

3.1.1. Multiple leaf switch. If the electrocaloric refrigerator has a cooling power of 1 watt at 4 K, Carnot operation requires a heat transfer of about 4 watts to the 15 K reservoir. Since the projected refrigerator has an efficiency in the range of 50 to 80% Carnot, a switch conductance k of at least 5 watts/K is desirable. Mechanical switches consisting of two metal surfaces pressed together[5] are commonly used at liquid helium temperatures for calorimetry experiments. Unfortunately, most of these switches have conductances of only a few milliwatts. However, Berman and Mate[6] have made measurements on gold-gold contacts for which $k \cong 0.2$ W/K at 4 K when closed by a 43 kg force prior to cooling. Their data extrapolates to about 1 W/K at 15 K, so a 5 watt/K heat switch could be feasible.

Increasing the closing force F increases the conductance[6] about as $F^{3/4}$. This means at least a 400 kg force is required for a 5 watt/K conductance. This much force is undesirable because the force must be transmitted into a dewar and also a high closing force increases the chance the switch contacts will be damaged by cycling.

A means of attaining a high conductance without an increase in closing force is shown in Fig. 7. The details of the switch are contained in the figure caption. A number of contact points are stacked in parallel so that a single clamping mechanism closes all. When the clamp is removed entirely,

the natural spring of the switch leaves move them slightly apart. Small closing forces may remain when leaves remain touching due to the stiffness of the leaves.

Conductance measurements on three switches are included here. Switch 1 had 13 leaves which were made of copper with a resistivity ratio of 500. The leaves were about 0.33 mm thick, 8-1/2 mm wide and 25 mm long from the base block to the contact point. The contact ends of the leaves were plated with about 2.5×10^{-3} mm commercial gold plating and the other end was soldered into the base block with pure indium.

Switch 2 had only 3 leaves. The leaves were again copper but with a resistance ratio of almost 1900. They were 0.75 mm thick, about 10 mm wide and 18 mm long from base block to contact point. The contact ends were plated with pure gold to a thickness of about 8×10^{-3} mm and they were again soldered to the base block with pure indium. The leaves were polished before plating.

Switch 3 also had 3 leaves but the leaves were silver with a resistivity ratio of 1400. The conductance of silver contacts has been measured[7] at 77 K and found to be better than gold. The dimensions and installation of the silver switch was the same as the second plated copper switch except that the contacts were polished but not plated.

For all three switches a resistivity ratio has been specified for the leaf material. This ratio is the electrical resistance at ambient temperature divided by the electrical resistance at 4 K. These ratios were measured using narrow strips of the actual leaf switch material after it had been rolled to size and annealed. All the leaves were rolled from round rods 1/4" or 3/8" in diameter.

The best contact conductances were obtained after cleaning the contact surfaces with a commercial copper cleaning powdered soap, rinsing with distilled water, washing with freon liquid and then drying with freon gas.

The temperatures of the first switch were measured using two carbon thermometers, calibrating one against the other. Switches 2 and 3 used the same carbon thermometers calibrated against a Ge thermometer. Calibration was accomplished by heating the helium heat exchanger with the switch closed. The thermometers are presumably in equilibrium. The thermometers were calibrated at three temperatures between 4 and 15 K and the measured resistance R at temperature T used to determine the constants A, B, and P of the equation

$$\log R = A + BT^{-P} .$$

The temperatures are computer calculated using this equation.

The conductance of the switch from base block to base block is the desired quantity so the thermometers were usually mounted on these blocks. Some measurements were made with the thermometers on the outer leaves as shown in Fig. 7. This permitted the conductance of just the contact points to be determined more accurately since the only correction to the measured temperature drop ΔT required was for the ΔT due to the finite conductivity of the leaves between the thermometer connection point and the contacts.

Data were taken by adjusting the needle valve H, Fig. 7, to fix the heat sink temperature at the desired value while heat was being applied at the other end of the switch. The temperatures and heater powers were recorded when the temperatures became stable.

Results of conductance measurements on the switches are shown in Fig. 8. The numbers 1, 2, and 3 on the points and curves refer to switches 1, 2, and 3. This is true also for Fig. 9 where the results here are compared to those of Berman and Mate for solid gold contacts. The conductance of the switch cooled closed by a 43 kg force is compared to the result of Berman and Mate in Fig. 9. The conductance is 1/4 that of their measurements. The overall switch conductance per contact is shown by curve 1A, Fig. 8. At an

80 kg closing force the conductance per contact is ~ 0.1 W/K and the total switch conductance is ~ 1.2 W/K.

The conductivity of a leaf from this switch was measured and found to be about 160 W/cmK in reasonable agreement with the resistivity ratio. The conductance of the indium solder joint was estimated from these measurements to be about 10 W/K cm^2.

The commercial gold plating solutions contain small amounts of cobalt or silver to harden the plating. This hardening is not desirable for pressed contacts and could reduce the contact conductance, hence pure gold was tried on switch number 2.

Switch number 2, described above, was tested next. The results for this switch are the curves and points 2 in Figs. 8 and 9. This switch was built with only 3 leaves so the contact conductance could be more directly measured. The conductance of this switch improved with increasing force after the switch was cooled closed as is shown in Fig. 8, curve 2. In order to compare with Berman and Mate at 43 kg closing force, it is necessary to extrapolate down from a 54 kg closing force. Extrapolating back to a 43 kg force using the relationship[6] $k \propto F^{3/4}$ gives a value of $k = 0.93$ W/K, in good agreement with the extrapolation of Berman and Mate's results to higher temperatures.

Curve 2A of Fig. 8 shows results of a measurement of the contact conductance These data were taken after cycling the switch between 1 and 51 times while cold. There appears to be no degradation due to cycling. However, the contact conductance is reduced to slightly less than 1/2 after opening and closing while cold.

Figure 8 curve 2B shows the conductance from base block to base block. The thermometers are mounted about 7 mm down the blocks from the attaching point of the leaves. The conductance of these blocks is sufficiently

poor that a correction of 0.24 K was subtracted from the measured ΔT. This correction was applied because the use of high purity copper base blocks for an actual switch application would remove most of this temperature drop.

The contact conductance of this switch was probably highest of all the measurements made. Because of the thermometer positions, the corrections that must be applied to find the contact conductance are sufficiently large and uncertain as to make a reasonably accurate determination of this conductance impossible. The contact conductance would be larger than that shown by curve 2A. The variation in conductance from run to run suggests that a more reliable cleaning technique is required for the contact surfaces.

The upper curve, 2B, shows the conductance of the switch as the closing force is reduced. The hysteresis may be due in part to mechanical drag but a large portion seems to be in the contact itself. Once the leaves are forced together the contact is better at all lower forces. This may imply a plastic deformation of the leaves or perhaps just a disturbance of the surface dirt.

The contact conductance of switch 2 cannot be represented simply by the closing force to some power as suggested by Berman and Mate[6]. The conductance dependence on force falls more rapidly with increasing force.

The conductance of switch 3 is a little less than switch 2 and the force dependence is less. The data points taken could as well have fit a straight line. A measurement of contact conductance was made at 4.5 K, curve 3B. From 3A and B conductance as a function of T can be estimated, Fig. 9, curve 3, which agrees in slope with Berman and Mate. This curve is for a closing force of 54 kg. At 43 kg force the conductances would be reduced about 20%.

The conductance of a switch must be sufficiently lowered when open. This switch must conduct well at 16 K with about a 1 K drop and conduct at least a factor of 30 less heat when open with about 12 K across it. The

on to off ratio for this switch is defined as 30. This minimum ratio is based on a one second cycle time and must be increased if the refrigerator cycle is slower. This on to off ratio would be around 300 if defined in the normal way.

The on to off ratio has been measured twice for switch 3 during different runs and in terms of the ratio defined above was found to be 84 and 270. Apparently contacts were touching with greater force due to poor alignment during the first measurement. This ratio may be smaller for multi-leaf switches because the chance of touching is greater.

The primary thrust of this work was to determine whether high conductance contact heat switches could be made that could be opened and closed cold without significantly degrading the heat transfer. This seems possible up to a total conductance of 5 W/K with a closing force less than 100 kg.

3.1.2. Helium gap switch. In order to transfer heat across contacts in a vacuum (previous section) large forces are required. A second mechanical switch under study uses a low pressure of helium gas around the contacts to provide good heat transfer without using high contact forces. The thermal conductivity of helium gas is independent of pressure until the pressure becomes so low that the mean free path of the molecules becomes comparable to the gap spacing. For a pressure of 1 torr the mean free path of helium gas is 1.1 μm at 4 K and 2.1 μm at 15 K. Therefore, for a gap of 5 μm or more the thermal conductivity of the gas will be the classical bulk value. The thermal conductance across the helium gap is simply

$$K = kA/\ell,$$

where k is the thermal conductivity of the helium, A is the cross sectional area of the gap, and ℓ is the gap spacing. The conductance can then be varied by changing the gap spacing. For the "on" case the two copper surfaces are brought into light contact. For reasonably smooth surfaces, the average gap spacing may be about 5 μm. The "off" condition is achieved by separating the two plates by a gap of about 5 mm. The conductance then decreases by a factor of 1000. For a ΔT of 11 K in the off case, the switch ratio would be $\ell_{off}/11\,\ell_{on}$ for k independent of temperature. Actually k varies from 0.084 mW/cm K at 4 K to 0.22 mW/cm K at 15 K[8], so the switch ratio becomes $\ell_{off}/7.5\,\ell_{on} = 133$ for the upper switch and $\ell_{off}/19.4\,\ell_{on} = 52$ for the lower switch as ℓ changes from 5 μm to 5 mm. The biggest uncertainty is the "on" conductance since the spacing depends on the quality of the surfaces. In order to transfer 5 watts at 15 K with a ΔT of 1 K, a surface area of 11.4 cm^2 is required with a gap of 5 μm.

An apparatus to test the heat conductance across a helium gap has been designed and built. Figure 10 shows a cross-sectional view of the test cell. The position of the movable plate is adjusted by a micrometer screw at room temperature. Thermal contact between the movable plate and the reservoir is made via 5 coaxial copper tubes which have gaps of about 50 μm. This allows a test of a movable heat link using helium gas.

An actual working heat switch can be made much simpler than this test device of Fig. 10. The switch is to have a cycle time of about 1 second so that the heat absorbed from one surface during the first half second can actually be stored in a movable plate with a high heat capacity. During the next one half second the plate is moved to make contact with the upper reservoir and transfers its stored heat to it. Thus no coaxial cylinders are required and a simple solenoid could move the plate from one position to the other. A 200 g movable plate of lead could be used for an upper switch but a lower switch would require as much as 8 kg of lead. Thus such a helium gap heat switch would only be practical for the upper switch.

The test apparatus in Fig. 10 will also be used to measure the conductance as a function of gas pressure for a fixed gap spacing. When the mean free path becomes comparable to the gap spacing, then the heat transferred is directly proportional to the pressure. Therefore a heat switch could be made where the gap spacing is about 50 μm and the gas pressure is varied from about 5×10^{-2} torr for the "on" case to about 10^{-5} torr in the "off" case. Such a switch has been tested by Gifford, et al.[9] Though this mode of operation would be difficult with a 1 second cycle time, it has the advantage that two gas valves could control a large number of refrigeration stages in which heat is pumped from the coldest stage to the warmest stage.[10]

3.2 Magnetothermal Switches (R. Radebaugh and J. D. Siegwarth)

The thermal conductivity of a metal is composed of the lattice and the electronic term, i.e., $k = k_\ell + k_e$. The electronic contribution can be reduced considerably in many metals by the application of a transverse magnetic field. The amount of reduction is proportional to the electrical magnetoresistive effect. Figure 11 shows a reduced Kohler diagram[11] of the transverse magnetoresistivity of most metals which is very helpful in selecting those metals with high magnetoresistive effects. A high magnetoresistive effect also reduces the eddy current heating. However, additional conditions must be met to obtain a large change in thermal conductivity with a magnetic field. The zero field thermal conductivity, which should be high, is proportional to the residual resistivity ratio (RRR = ρ_{295}/ρ_o), where ρ_o is usually measured at 4.2 K. The lattice thermal conductivity, which should be low, is given theoretically by the expression[12]

$$k_\ell = \frac{3.1 \times 10^2 k_\infty}{G N_o^2 \theta_o^2} T^2 \text{ (W/cm K)},$$

where k_∞ is the constant thermal conductivity at high temperatures, e.g., room temperature, G is a numerical factor which is about 70, N_o is the number of free electrons per atom, and θ_o is the Deby temperature at 0 K. From this expression it is obvious that a high θ_o will give a low k_ℓ. The important properties of a metal which would make a good heat switch are summarized as follows:

(1) high magnetoresistive effect

(2) high residual resistance ratio (RRR $\geq$ 1000)

(3) high Debye temperature, $\theta_o \geq 300$ K.

Even though some materials, such as bismuth, have extremely high magnetoresistive effects, they are no good as heat switches since they do not satisfy conditions (2) and (3) above. Table I lists the various metals which are known to satisfy all three conditions above and therefore would be potential heat switch materials.

Table 1. A summary of metals which have the potential for making good magnetothermal heat switches in the 4 - 15 K range. The metals are listed in order of decreasing magnetoresistive effect.

Metal	highest RRR to date	θ_o (K)	sufficient data on k(T,H) exists
Ga	2×10^5	324	yes
Be	3×10^3	1160	no
Mg	$10^6 - 10^7$	342	no
W	3×10^4	405	yes
Fe	2×10^3	464	no
Ru	$> 10^3$	600	no

Of the six possible candidate materials only Be and possibly Ru have high enough θ_o to be potentially useful as the upper switch where the "on" temperature is about 15 K. The other materials would be useful only for the lower switch where the "on" temperature is 4 K. Only Ga and W have been measured in enough detail to predict the heat switch performance. In fact Ga has already been used as a heat switch in the 1-4 K temperature range.[13] Our first efforts were then to make a switch of Ga.

3.2.1. Gallium. Figure 12 shows the behavior of the thermal conductivity of gallium as a function of temperature for various transverse magnetic fields. The H = 0 curves are from the work of Boughton and Yaqub[14], and the $H \neq 0$ curves are from Engels, et al.[13]. In the "off" state of the switch ($H \neq 0$) the temperature will be 15 K on one side of the switch and 4 K on the other side. The heat flow must be evaluated by integration over the k (T) curve. For $k \propto T^2$ the average conductivity is the value of k at about 11 K. For the lower switch, the switch ratio is then approximately $(1/11)k_4/k_{11}$ and for the upper switch the ratio is $(1/11)k_{15}/k_{11}$. Table 2 lists these switch ratios for gallium as well as for several other metals.

Table 2. Estimated thermal conductivity at three different temperatures and the switch ratio for several heat switch metals. Units for k are W/cm K.

Metal	H = 0 k (4 K)	H = 0 k (15 K)	H = 14 k Oe k (11 K)	Switch Ratios lower	Switch Ratios upper
Gallium	200	5.0	0.20	91	2.3
Beryllium	90	~200	0.035	234	520
Magnesium	~800	~115	0.2 - 0.5	145 - 360	21 - 52
Tungsten	800	115	0.45	162	23
Iron	50	70	~0.5	9	13
Ruthenium	50	80	0.1 - 0.3	15 - 45	24 - 73

Two gallium magnetothermal heat switches were made by growing a single crystal of 99.9999% Ga in a teflon mold like that described by Yaqub and Cochran[15]. Each crystal had relatively large diameter discs grown on each end to reduce the thermal resistance at the bond between gallium and copper. Both crystals broke upon cooldown. The first was subject to slight tension from the stainless steel support system, whereas the second was subject to compression from the teflon support system. Because of the brittleness and low melting point (29.9°C) of gallium, and because of the encouraging results now being obtained with beryllium, we are suspending further work on gallium.

3.2.2. Beryllium. Figure 13 shows the expected thermal conductivity of beryllium with a resistance ratio of 3000 in both zero magnetic field and in sufficiently high magnetic fields to suppress the electronic conduction. Until now the only measurements of the thermal conductivity of beryllium in a magnetic field were those of Grüneisen[16,17], which are shown in Fig. 13. His sample had a resistance ratio of 780. He found that the maximum field effect occured with the heat flow along the hexagonal c axis and the magnetic field along an a axis such as $(11\bar{2}0)$. Unfortunately his measurements were made at only 23.5 K and 81 K. The estimated lattice conductivity is based on measurements of the thermal conductivity of beryllium alloys[18,19].

Since beryllium shows great promise as a heat switch, we decided to measure k (T, H) for the unknown region below 23.5 K. Two samples of beryllium have been received. One is disc shaped and its resistance ratio was measured to be 72. That sample was given to us by Dr. S. K. Sinka of Iowa State. The other sample was a 3 mm square rod, 25 mm long. This sample is on loan to us from Dr. R. Soulen of NBS, Washington, who in turn received this from Dr. W. Reed of Bell Laboratories. According to Dr. Reed, the resistance ratio of the sample should be between 1000 and 3000, though we have not measured this yet. The orientation of both crystals we determined from back scattered x-ray Laue photographs. The hexagonal c axis is in the plane of the disc sample and along the long axis of the other crystal. According to the work of Grüneisen[16,17], this orientation gives the maximum field effect.

The 3 mm square by 25 mm long crystal was mounted in a specially constructed thermal conductivity apparatus which would fit between the poles of an electromagnet. A varnish was used to attach one end of the sample to the reservoir and a heater to the other end. Indium solder would have provided much better thermal contact but we were not allowed to solder to this borrowed sample. Two 1/8 watt Allen Bradley carbon thermometers with flats ground on one side were varnished on one side of the sample a distance of 12.5 mm apart. Attached

to the reservoir were a calibrated germanium thermometer and a capacitance thermometer[20]. These thermometers were used to calibrate the carbon thermometers in a zero magnetic field and in magnetic fields, respectively. The thermal conductivity was measured from about 1.7 K to 30 K in transverse magnetic fields of 0, 1, 2, 4, 6, 10, and 12 k 0e. In addition the thermal conductivity at 4 K in a 10 k 0e field was measured as a function of the angle of rotation of the magnetic field. This rotation diagram was used to find the a axis of the crystal. Computer programs to analyze all of the data are in the final assembly stages. However hand calculated points for the H = 12.0 k 0e data lead to the curve shown in Figure 13. The high temperature end agrees well with the data of Grüneisen and Adenstedt[16]. The measured ΔT for H = 0 was so small that the data is virtually impossible to analyze by hand calculations. The value of k in H = 0 at 4 K is essentially determined by the resistance ratio. According to Dr. W. Reed a resistance ratio of even greater than 3000 could be obtained without too much difficulty. One disturbing point is that the H = 0 data of Grüneisen and Adenstedt shows a negative deviation from the theoretical curve at about 20 K, whereas all other metals show some positive deviation. The estimated switch ratios for beryllium are shown in Table 2.

3.2.3. Tungsten. The magnetothermal conductivity appears to be quite well characterized from the measurements by de Haas and de Nobel[21] and by Long[22]. Figure 14 shows the thermal conductivity behavior and Table 2 gives the expected switch ratios.

3.2.4. Magnesium. At present we have a rather small crystal of magnesium with a resistance ratio of 27,000. This was given to us by Dr. S. Shultz of the University of California in La Jolla. Its small size would make thermal conductivity measurements quite difficult. We have been negotiating with Dr. R. W. Stark of the University of Arizona to obtain one of their Mg crystals with RRR $\sim 10^6$ - 10^7 which is the purest metal in the world. His crystals have already been cut into 2 mm square rods with copper evaporated on the ends for making solder contact. They have already measured the electrical magnetoresistivity of these samples[23].

4. THERMAL CONDUCTANCE OF JOINTS (R. Radebaugh)

Any low temperature apparatus will be composed of many parts. In the electrocaloric refrigerator there will be a 15 K reservoir, refrigeration element, heat switches, and load. Each of these parts must be joined together in some fashion that will allow large amounts of power to be transferred between these parts. An improperly designed joint may have a thermal resistance at the joint which could be larger than most other resistances in the system. The electrocaloric refrigerator has a cyclic operation mode so that the mass of material connected to the cyclic element must be kept small enough to prevent its heat capacity from thermally overloading the system. This is accomplished by using a small amount of high purity copper for the transfer of heat. The small volume of copper means that the surface area of the joints will be quite small and therefore may have high joint resistances.

Figure 15 is a compilation of existing data on the thermal conductance of solder joints, grease joints, and pressure joints. In the case of the pressure joints the thermal conductance, in units of W/K, is for the whole joint, independent of the surface area. For the grease and solder joints the thermal conductance is for 1 cm^2.

The curves shown in Fig. 15 are taken from the following references:

Solder joints ($T < 1$ K): ref. 24, 25

Solder joints (1 K $< T <$ 4 K): ref. 26, 27

Solder joints (room temperature): 28

Grease and adhesive joints: 24, 29, 30, 31, 32

Pressure contacts: 31, 32, 5, 6, 33

It is rather amazing that there is no data on the thermal conductance of solder joints in the region between 4 K and room temperature. But rough interpolations (shown by the dashed lines in Figure 11), based somewhat on values of the bulk thermal conductivity of certain solders, suggest that solder joints are superior to all other joints in the region above 4 K. Even then a conductance of about 10 W/cm^2K means that the joints must have more than 1 cm^2 to transfer 5 W of power with a ΔT much less than 1 K.

Because of the importance and uncertainty of joint thermal conductance we plan to measure the thermal conductance of a few solder joints. Indium solder holds promise of having a higher conductance than any of the alloy solders. Thus we plan to study indium in particular. We recommend that a much larger program be undertaken to study the thermal conductances of joints, especially solders. We have neither the time nor the money to investigate this problem in full detail in this electrocaloric refrigerator program. The thermal resistance at joints could become a serious problem whenever large heat loads are concentrated in a small region. Such would be the case as refrigerators are miniaturized.

5. REFERENCES

1. W. N. Lawless, "Dielectric Cooling Technology: 15 - 4 K", Proc. Cryocooler Conf., USAF, Oct. 1973, Tech. Report AFFDL-TR-73-149, Vol. 1, p. 417. See also U.S. Patent Nos. 3,436,924 and 3,638,440.
2. W. N. Lawless, "Three Application Areas for $SrTiO_3$ Glass-Ceramics" Ferroelectrics 3, 387 (1972).
3. W. N. Lawless, "Method for Measuring Specific Heat and Electrocaloric Coefficient, 2-20 K", submitted for NBS Tech. Note.
4. C. V. Heer, C. B. Barnes, and J. G. Daunt, Rev. Sci, Instrum. 25, 1088 (1954).
5. See for example J. H. Colwell, Rev. Sci. Instrum. 40, 1182 (1969) and the references contained therein.
6. R. Berman and C. F. Mate, Nature 182, 1661 (1958).
7. R. B. Jacobs and C. Starr, Rev. Sci. Instrum. 10, 140 (1939).
8. R. D. McCarty "Thermophysical Properties of Helium -4 from 2 to 1500 K with Pressures to 1000 Atmospheres", NBS Tech. Note 631, 1972.
9. W. E. Gifford, N. Kadaikkal, and A. Acharya, "Simon Helium Liquefaction Method Using a Refrigerator and Thermal Valve", Adv. Cry. Eng. 15, 422 (1970).
10. We are indebted W. E. Gifford for this suggestion.
11. G. T. Meaden, "Electrical Resistance of Metals" (Plenum Press, New York, 1965) p. 133.
12. H. M. Rosenberg "Low Temperature Solid State Physics" (Oxford at the Clarendon Press, 1963), p. 121.
13. J. M. L. Engels, F. W. Gorter, and A. R. Miedema, Cryogenics 12, 141 (1972).
14. R. I. Boughton and M. Yaqub, Phys. kondens. Materie 9, 138 (1969).
15. M. Yaqub and J. F. Cochran, Phys. Rev. 137, A1182 (1965).
16. Von E. Grüneisen and H. Adenstedt, Ann. d. Phys. [5] 31, 714 (1938).
17. Von E. Grüneisen and H. D. Erfling, Ann. d. Phys. [5] 38, 399 (1940).

18. R. L. Powell, J. L. Harden, and E. F. Gibson, J. Appl. Phys. 31, 1221 (1960).

19. G. K. White and S. B. Woods, Can. J. Phys. 33, 58 (1955).

20. W. N. Lawless, Rev. Sci. Instrum. 42 561 (1971).

21. W. J. De Haas and J. De Nobel, Physica 5, 449 (1938). J. De Nobel, Physica 23, 261 (1957).

22. J. R. Long, Phys. Rev. B3, 1197 (1971).

23. R. W Stark and C. B. Friedberg, J. Low Temp. Phys. 14, 111 (1974).

24. A. C. Anderson and R. E. Peterson, Cryogenics 10, 430 (1970).

25. W. A. Steyert, Rev. Sci. Instrum. 38, 964 (1967).

26. L. J. Challis and J. D. N. Cheeke, Proc. Phys. Soc., 83, 109 (1964).

27. L. J. Barnes and J. R. Dillinger, Phys. Rev. 141, 615 (1966).

28. M. M. Yovanovich and M. Tuarze, J. Spacecraft 6, 855 (1969); M. M. Yovanovich, J. Spacecraft 7, 1013 (1970).

29. T. Ashworth, J. E. Loomer, and M. M. Kreitman, Adv. Cry. Eng. 18, 271 (1973).

30. J. H. McTaggart and G. A. Slack, Cryogenics 9, 384 (1969).

31. H. J. Sauer, Jr., C. R. Remington, W. E. Stewart, Jr., and J. T. Lin, XI International Thermal Conductivity Conf., Albuquerque, N. M., 1971, p. 22.

32. H. J. Sauer, Jr., C. R. Remington, and G. A. Heizer, XI International Thermal Conductivity Conf., Albuquerque, N. M., 1971, p. 24.

33. E. Gmelin, Cryogenics 7, 225 (1967).

6. FIGURE CAPTIONS

Figure 1. Typical dielectric constant (DK) vs. temperature (TEMP) behavior for a multilayer sample of Code FEL. The measuring frequency is 1 kHz (F = 1000).

Figure 2. Dependence of the permittivity derivative $(\partial\epsilon/\partial T)_o$ at 4 K on crystallization temperature for various samples of $SrTiO_3$ glass-ceramics: "FEP Research Samples" are bulk samples; "FEP, FEL Multilayers" are manufactured samples; "FHJ-Warden" are samples from an alternate manufacturing process; "FHJ-AVC" are initial samples from a controlled-viscosity crystallization experiment; and "Boro-alumino-silicate (FHK)" are results obtained on a feldspar-free bulk sample (see text).

Figure 3. Increase in the breakdown field strength at 4 K with increasing dielectric thickness (see text).

Figure 4. Variation of thermal-link time constant τ with temperature for several machined Allen-Bradley radio resistors used with glass-ceramic samples. The curve labelled "Metal Link" illustrates the advantage of the graphite links. The 2.7 Ω - 1/2 W resistor was selected for the experiments.

Figure 5. Schematic drawing of an assembled and mounted sample for the combined specific heat-electrocaloric coefficient experimental method: (A) reservoir; (B) graphite thermal link; (C) strip of glass-fritted silver; (D) indium solder joint; (E) thermometer leads; (F) thermometer, ground 220 Ω - 1/8 W Allen-Bradley resistor; (G) heater wire bonded between two samples with GE 7031 varnish; (H) heater wire wrapped in sample; (I) heater leads tempered to reservoir. For voltage application, a high voltage lead is indium soldered to the bottom of the sample (not shown) and the reservoir is ground.

Figure 6. Thermal conductivity data on fused silica and three glass-ceramics.

Figure 7. Schematic of heat switch and actuating mechanism. The conducting parts of the switch are hatched.

The leaves (A,A) of either copper with free ends gold plated or silver are soldered into slots in OFHC copper base blocks B, B with pure indium. Carbon thermometers are either mounted on copper tabs indium soldered to top and bottom outer leaves C, C, or on the copper blocks as shown by D, D, since only two carbon thermometers are used at a time. A heater E is attached to the lower copper block to establish the desired heat flux. A germanium thermometer F is used to calibrate the carbon thermometers in place. A second heater (not shown) is attached to the upper block and used to heat the whole switch assembly during calibration. The upper base block B is thermally anchored to the flat circular heat exchanger (T). Liquid helium is admitted through needle valve H and the vapor is removed through the pump line and valve I. The line is jacketed to a point above the bath so the enthalpy of the gas as well as the latent heat can be used to cool the switch when measurements are being made above 4 K.

The switch is clamped shut by the two brass jaws J, J. The force is applied over an area of 3.2 mm times the leaf width, about 9 mm. The closing force is applied by an air piston K. The forces are transmitted through the wire L and a stainless steel tube M. The jaws are moved by two pairs of bell cranks N, N which are coupled to the pull wire L through an equalizing device P. The wire is heat sinked with copper braid at Q and vacuum jacketed so a sliding O-ring seal R can be placed at room temperature. The switch assembly is placed in a vacuum container S sealed by Woods metal joint near the top. The vacuum can is immersed in liquid helium in a set of glass dewars T.

Figure 8. Conductivities as a function of closing force for switches 1, 2, and 3. All curves and points are normalized to one contact. They are corrected to contact conductance only unless otherwise specified.

Switch 1: Point 1, cooled closed, heat sink approximately 15.2 K.

Curve 1, conductance from base block to base block after 1 and 75 cycles cold. Heat sink approximately 16 K.

Switch 2: Curve 2 switch cooled closed then force measured while cold. Heat sink approximately 14.4 K.

Curve 2A - The switch cycled from 1 to 51 times cold. Heat sink at about, 14.3 K.

Curve 2B - Base block to base block. Heat sink at about 14.3 K. Correction applied for conductivity of base blocks .51 cycles.

Switch 3: Point 3 cooled closed. Heat sink about 14.3 K.

Curve 3A switch cycled 1 to 155 times cold. Heat sink about 14.7 K.

Curve 3B switch cycled 155 times cold. Heat sink about 4.5 K.

Figure 9. T dependence of the conductance of one contact. Curve 4, data of Berman and Mate extrapolated to about 17 K. Closing forces are 43.0 kg unless otherwise specified.

Point 1. Switch 1 closed at ambient.

Point 2. Switch 2 closed at ambient.

Point 2A. Switch 2 closed cold.

Point 3. Switch 3 closed at ambient.

Curve 3A switch 3 closed cold with a 54 kg force.

Figure 10. A cross sectional view of the test apparatus to measure the behavior of a helium gap switch. The gap spacing can be varied as well as the helium gas pressure.

Figure 11. The transverse magnetoresitivity of 23 metals (Ru was added to original figure) on a reduced Kohler diagram from Meaden[11]. In this plot ρ_θ is the resistivity at the Debye temperature. Only those metals with relatively high $\Delta\rho/\rho$ have the potential for making good magnetothermal switches.

Figure 12. The thermal conductivity of single crystal gallium in transverse magnetic fields. The heat flow is parallel to the a axis and the field is parallel to the c axis. The thermal conductivity in zero field is somewhat size dependent because of the long electron mean free path.

Figure 13. The thermal conductivity of single crystal beryllium in transverse magnetic fields. The heat flow is parallel to the c axis and the magnetic field is parallel to the a axis. The data points are from Grüneisen and Adenstedt[16] on a sample with a residual resistance ratio (RRR) of 780. The estimated behavior of a higher purity sample (RRR = 3000) is also shown along with preliminary results of our measurements in a field of 12 kOe.

Figure 14. The measured thermal conductivity of single crystal tungsten in transverse magnetic fields[21, 22]. A size dependence occurs at low temperatures in zero field for the higher purity sample.

Figure 15. The thermal conductance of grease, adhesive, solder, and pressure joints as a function of temperature. The conductance is per cm^2 of contact for the grease, adhesive, and solder joints. However, the curves for the pressure joints give the total conductance of the joint, independent of the area, but dependent on the total force applied. The dashed lines are our estimates of the conductance in areas where no data exist.

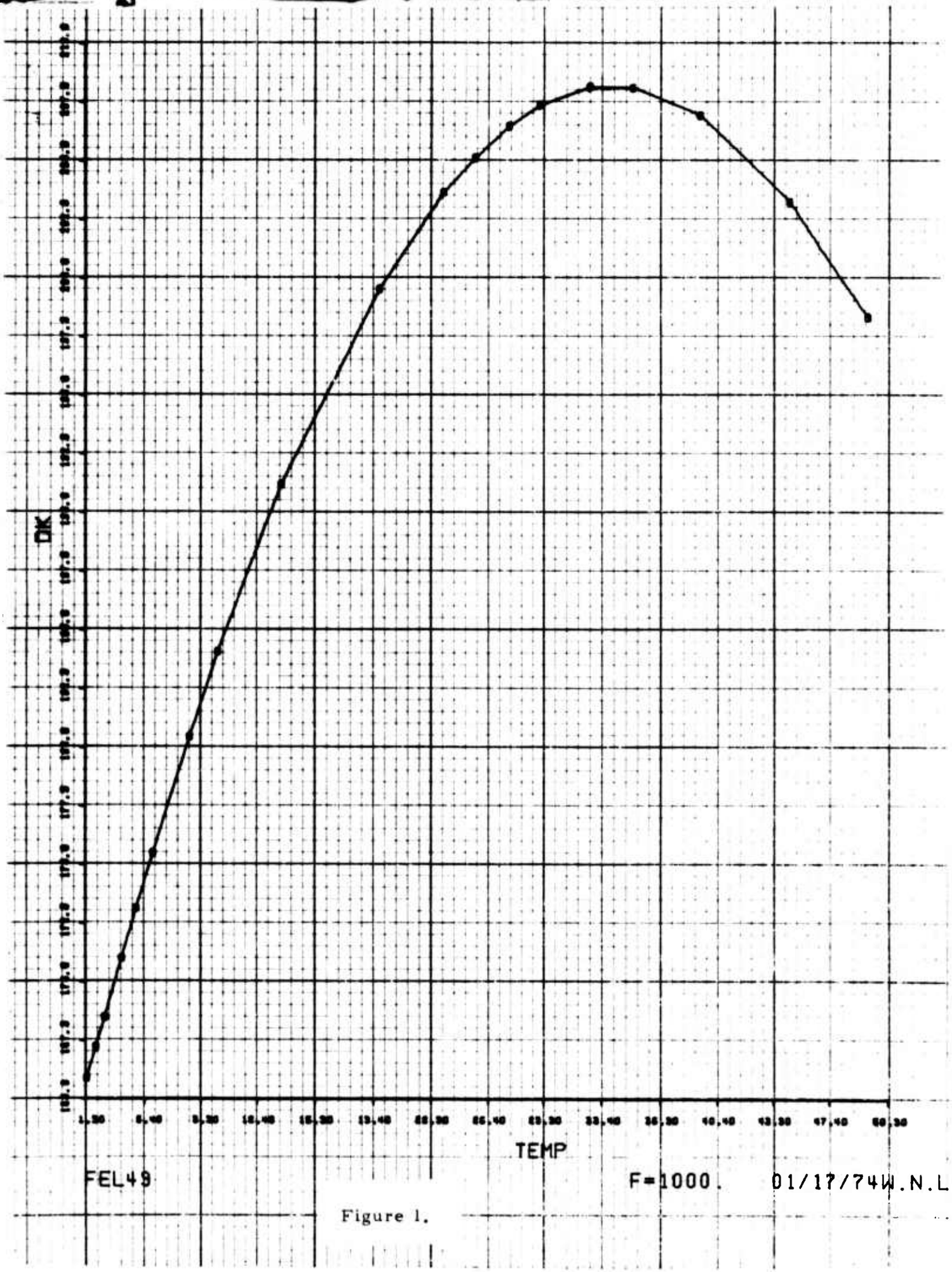

Figure 1.

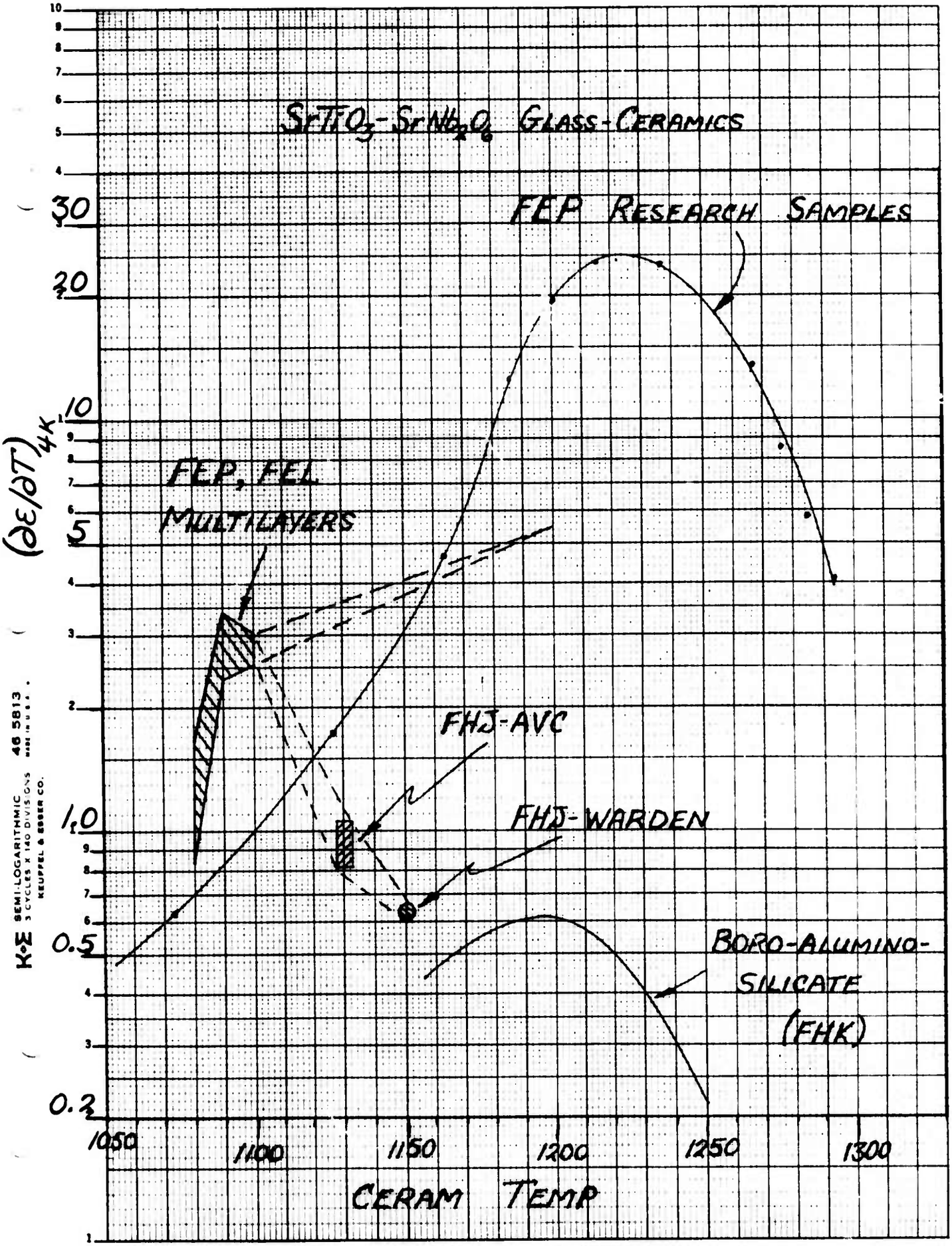
SrTiO3-SrNb2O6 GLASS-CERAMICS
FEP RESEARCH SAMPLES
FEP, FEL MULTILAYERS
FHJ-AVC
FHJ-WARDEN
BORO-ALUMINO-SILICATE (FHK)
(∂ε/∂T)4K
CERAM TEMP
1050
1100
1150
1200
1250
1300
30
20
10
5
1.0
0.5
0.2
K-E SEMI-LOGARITHMIC 46 5813
3 CYCLES X 140 DIVISIONS
KEUFFEL & ESSER CO.

Figure 2.

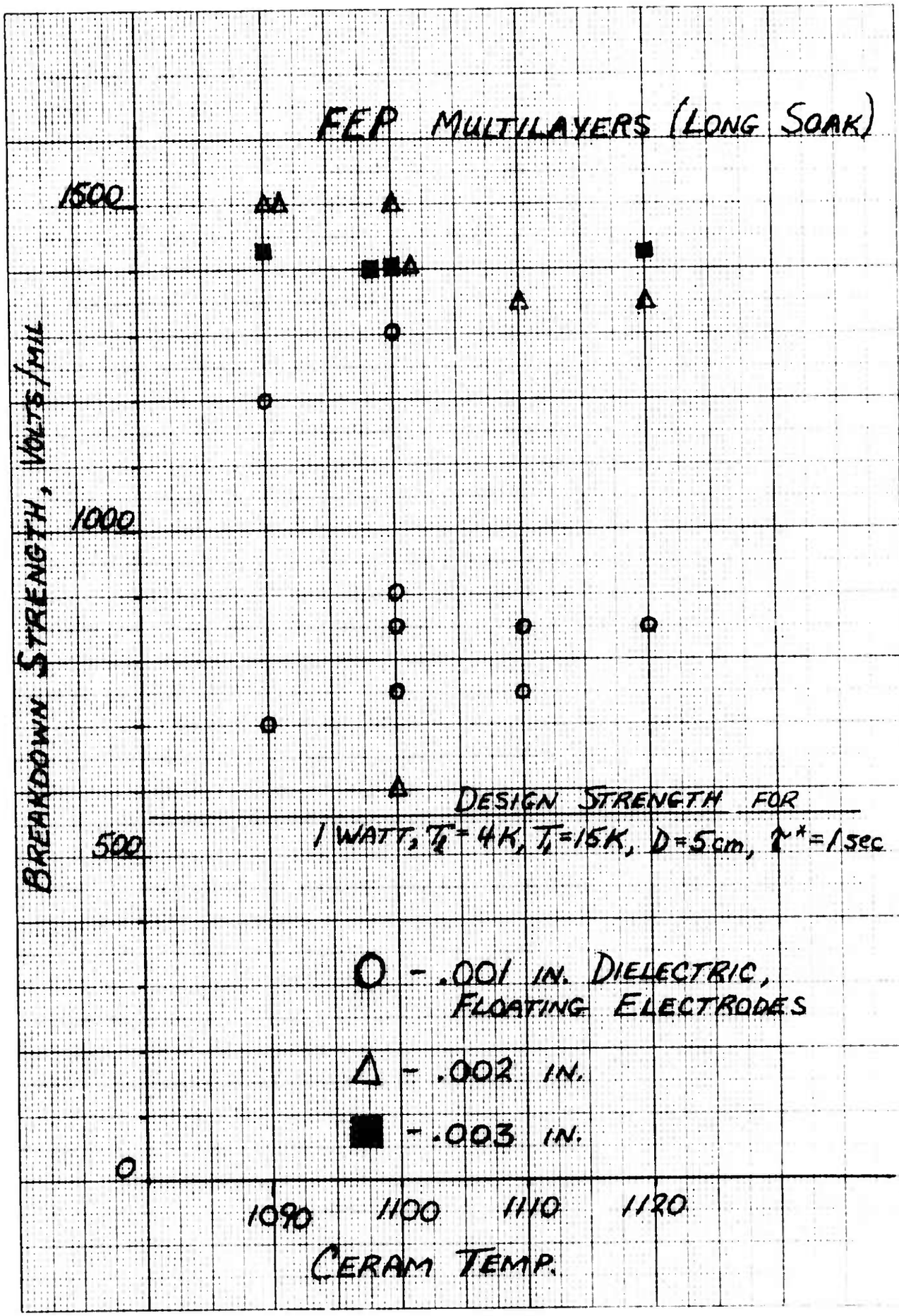
FEP MULTILAYERS (LONG SOAK)
BREAKDOWN STRENGTH, VOLTS/MIL
1500
1000
500
0
DESIGN STRENGTH FOR
1 WATT, T_2 = 4K, T_1 = 15K, D = 5 cm, τ^* = 1 sec
○ - .001 IN. DIELECTRIC, FLOATING ELECTRODES
△ - .002 IN.
■ - .003 IN.
1090
1100
1110
1120
CERAM TEMP.

Figure 3.

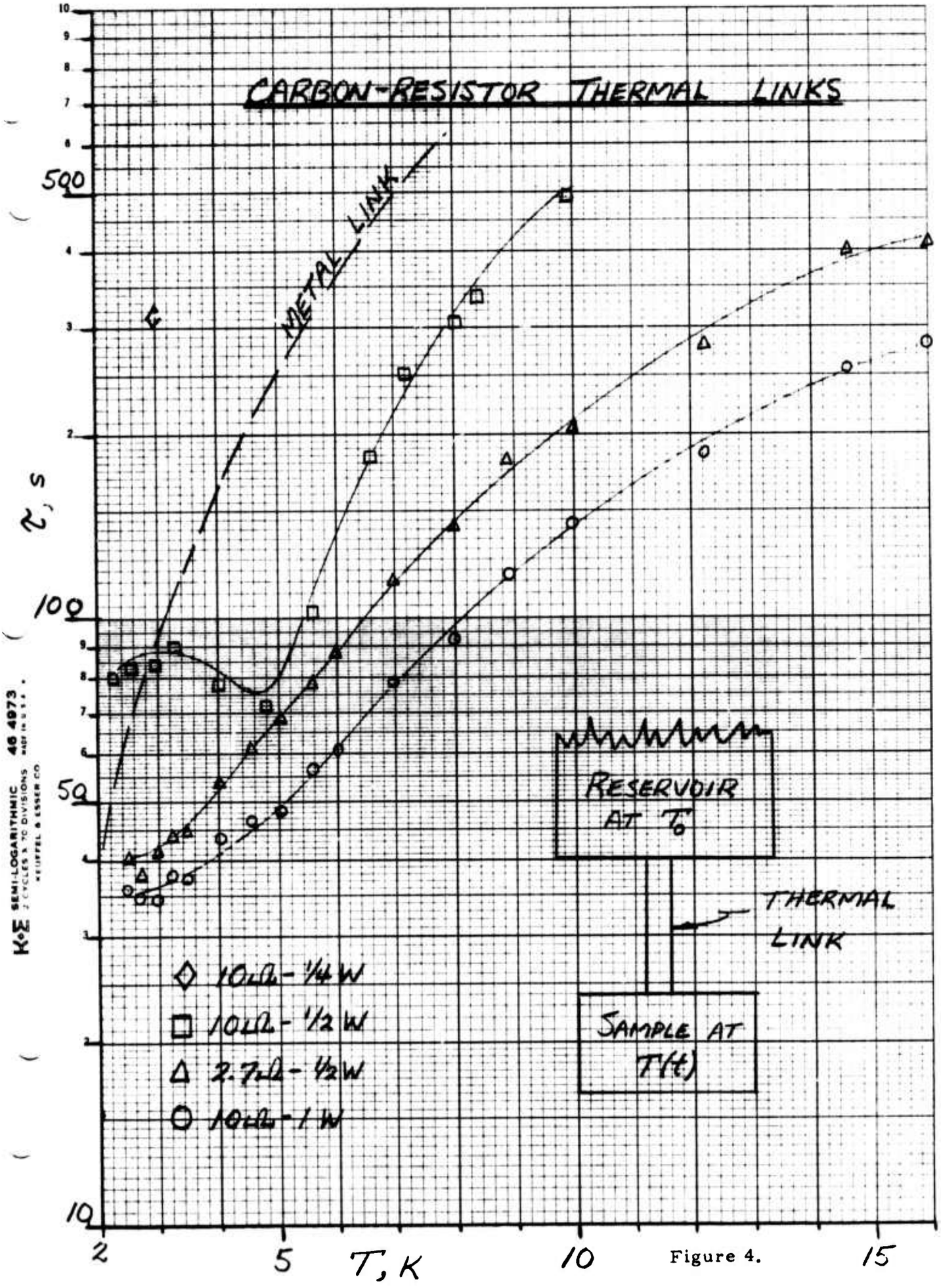
CARBON-RESISTOR THERMAL LINKS
METAL LINK
τ, s
T, K
RESERVOIR AT T₀
THERMAL LINK
SAMPLE AT T(t)
◇ 10Ω - ¼ W
□ 10Ω - ½ W
△ 2.7Ω - ½ W
○ 10Ω - 1 W
500
100
50
10
2
5
10
15

Figure 4.

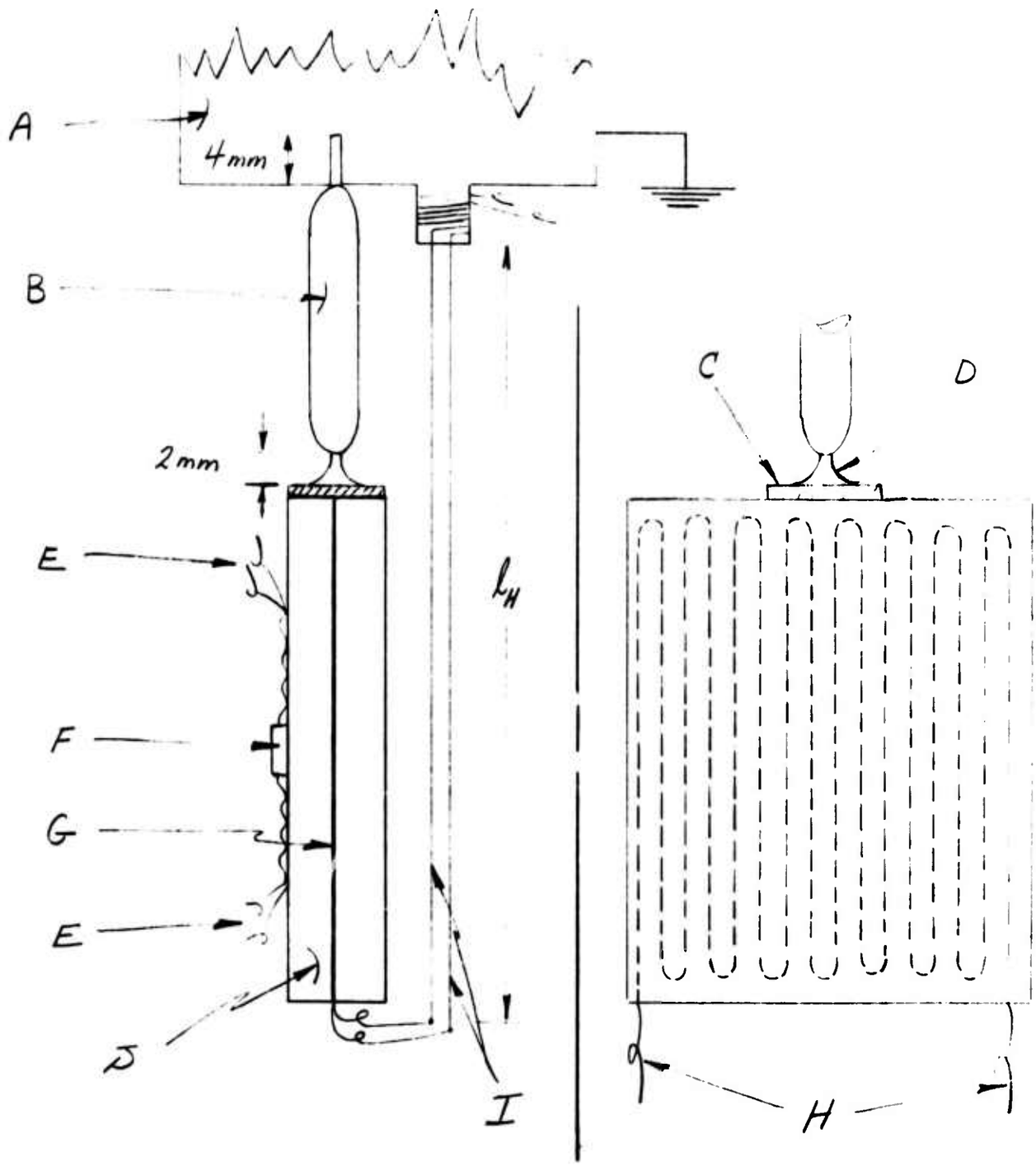

Figure 5.

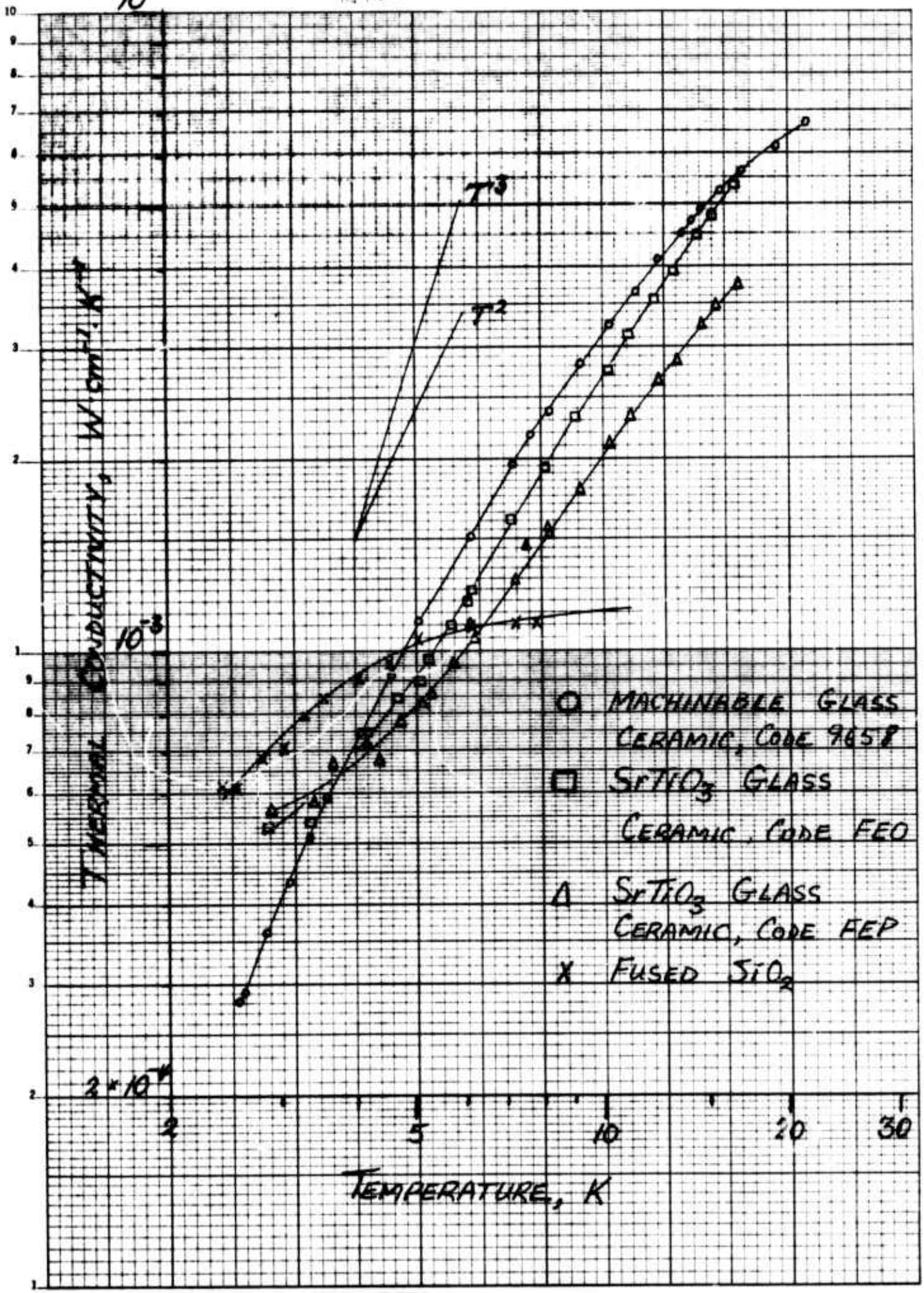
10^{-2}
T^3
T^2
10^{-3}
2×10^{-4}
THERMAL CONDUCTIVITY, W/cm°K
TEMPERATURE, K
2
5
10
20
30
MACHINABLE GLASS CERAMIC, CODE 9658
$SrTiO_3$ GLASS CERAMIC, CODE FEO
$SrTiO_3$ GLASS CERAMIC, CODE FEP
FUSED SiO_2

Figure 6.

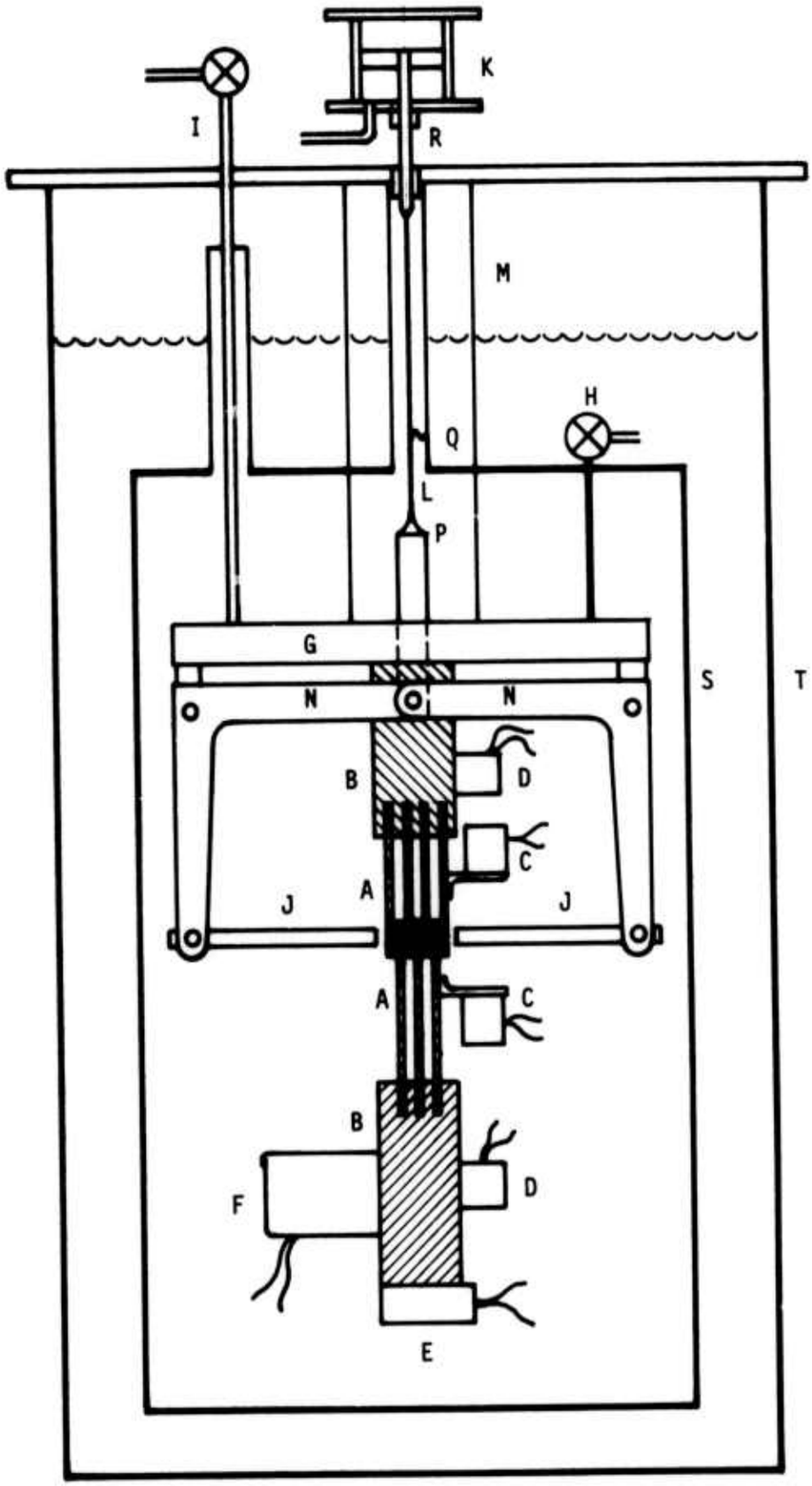

Figure 7.

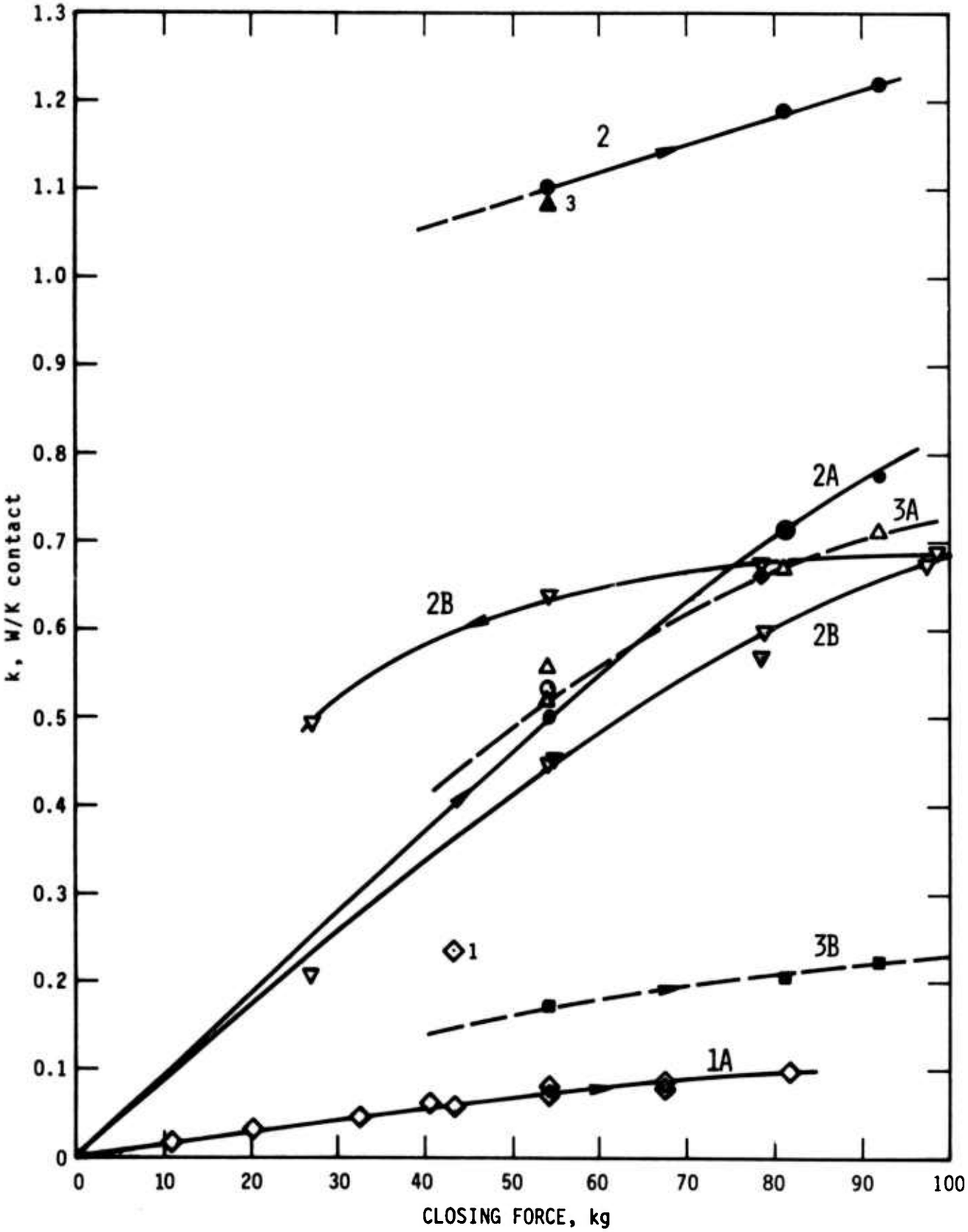
k, W/K contact
CLOSING FORCE, kg
1.3
1.2
1.1
1.0
0.9
0.8
0.7
0.6
0.5
0.4
0.3
0.2
0.1
0
0
10
20
30
40
50
60
70
80
90
100
2
3
2A
3A
2B
2B
1
3B
1A

Figure 8.

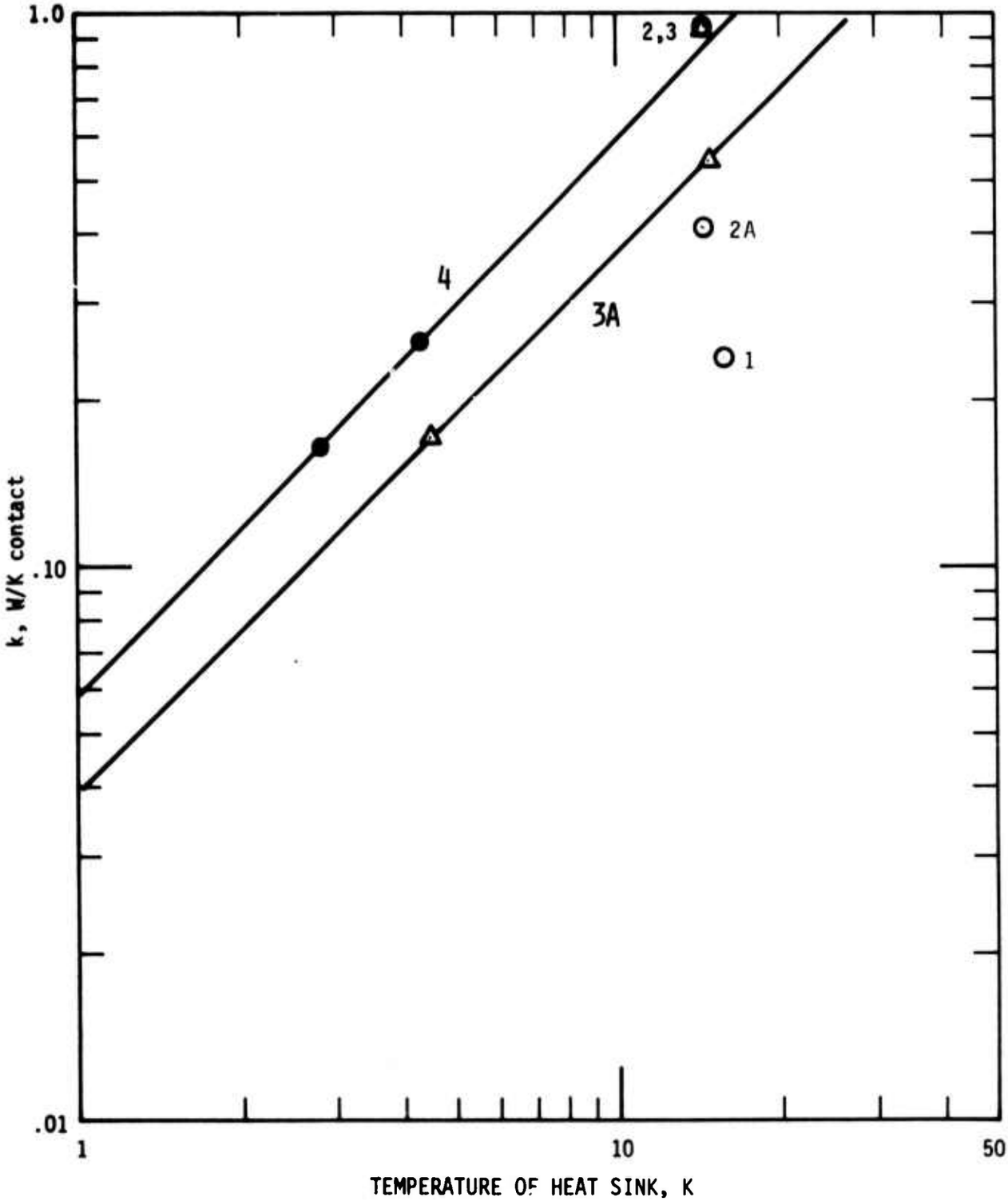
1.0
.10
.01
k, W/K contact
1
10
50
TEMPERATURE OF HEAT SINK, K
2,3
2A
4
3A
1

Figure 9.

NATIONAL BUREAU OF STANDARDS, CRYOGENIC ENGINEERING LABORATORY
LABORATORY NOTE

PROJECT NO.	FILE NO.	PAGE
2751481		1

SUBJECT

HELIUM GAP HEAT SWITCH

NAME Ray Radebaugh
DATE Sept. 27, 1973

(Actual size)

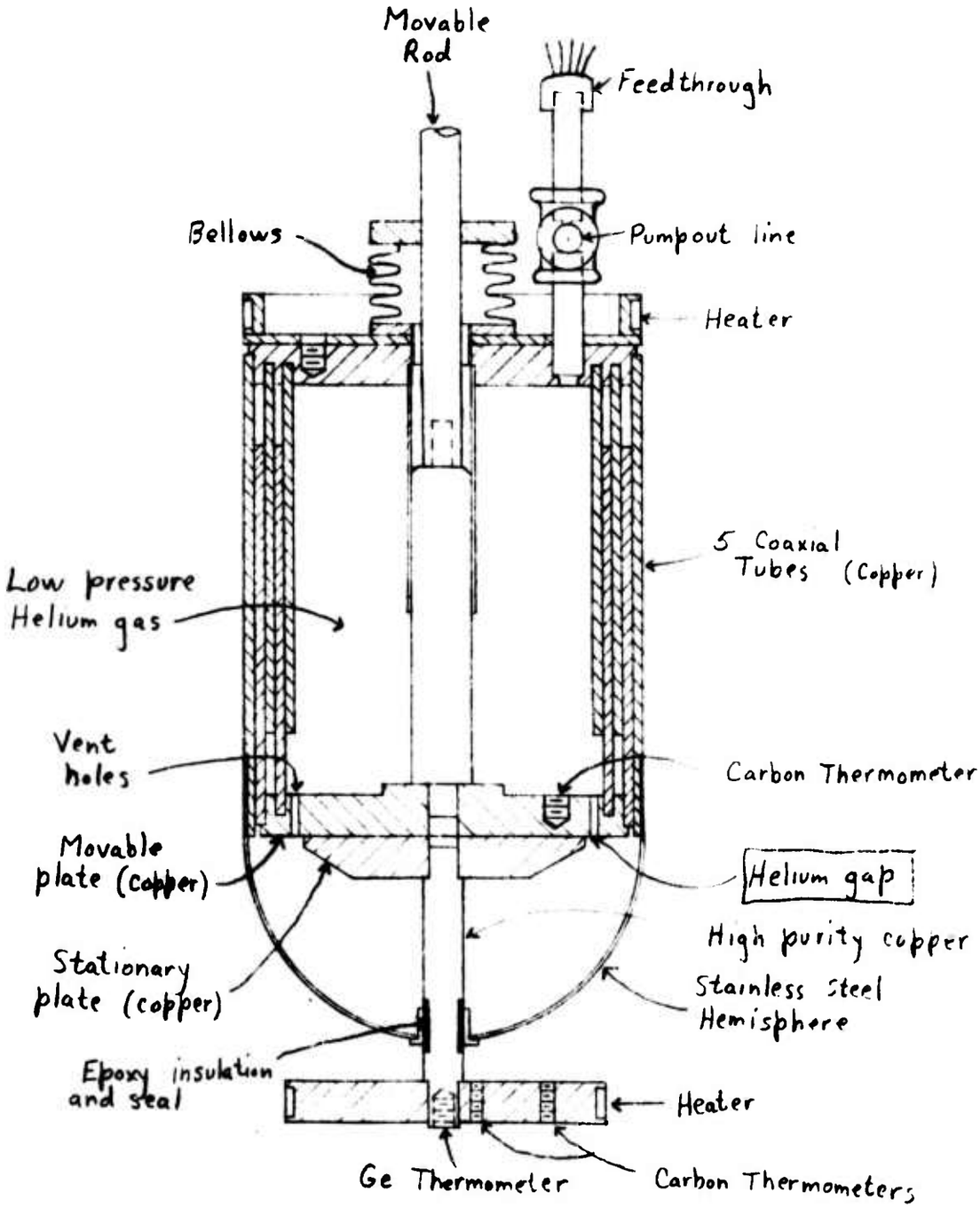

Figure 10.

GOULVIE PRESS, INC., BROOKLYN 17, N. Y. STOCK NO. 450

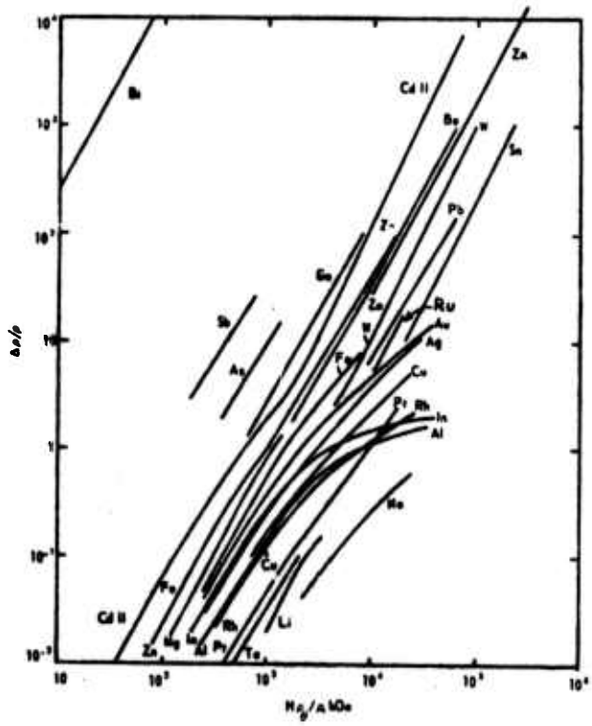

Fig. 46. The transverse magnetoresistivity of 22 metals plotted on a reduced Kohler diagram (taken from Olsen[36] and based on the results of Justi and Ascher-man[232] and Luthi[282]).

For a particular metal, f depends on the orientation of H and E, and, if a single crystal, also on the orientation of the crystal axes. Theoretically, Kohler's rule can be shown to follow directly from the Boltzmann equation, if a relaxation time solution can be employed; and experimentally it is usually found to agree fairly well with observation. Figure 46, given to illustrate it, with $H\rho_\theta/\rho$ as abscissa (where ρ_θ is the resistivity at $T = \theta_D$°K), is called a *reduced Kohler plot* (Justi[231]). By using it, a rough estimate of the transverse magnetoresistivity may be deduced if, at any temperature T_1, ρ_{T_1}, ρ_θ, and H are known. From the parameters in Kohler's rule, we note that in order to obtain as large a $\Delta\rho/\rho$ as possible for a given metal we must employ *pure* metals at low temperatures (to lessen ρ) and high fields. We note also that the magnetoresistivity effect is smallest in the simplest alkali metals

Figure 11

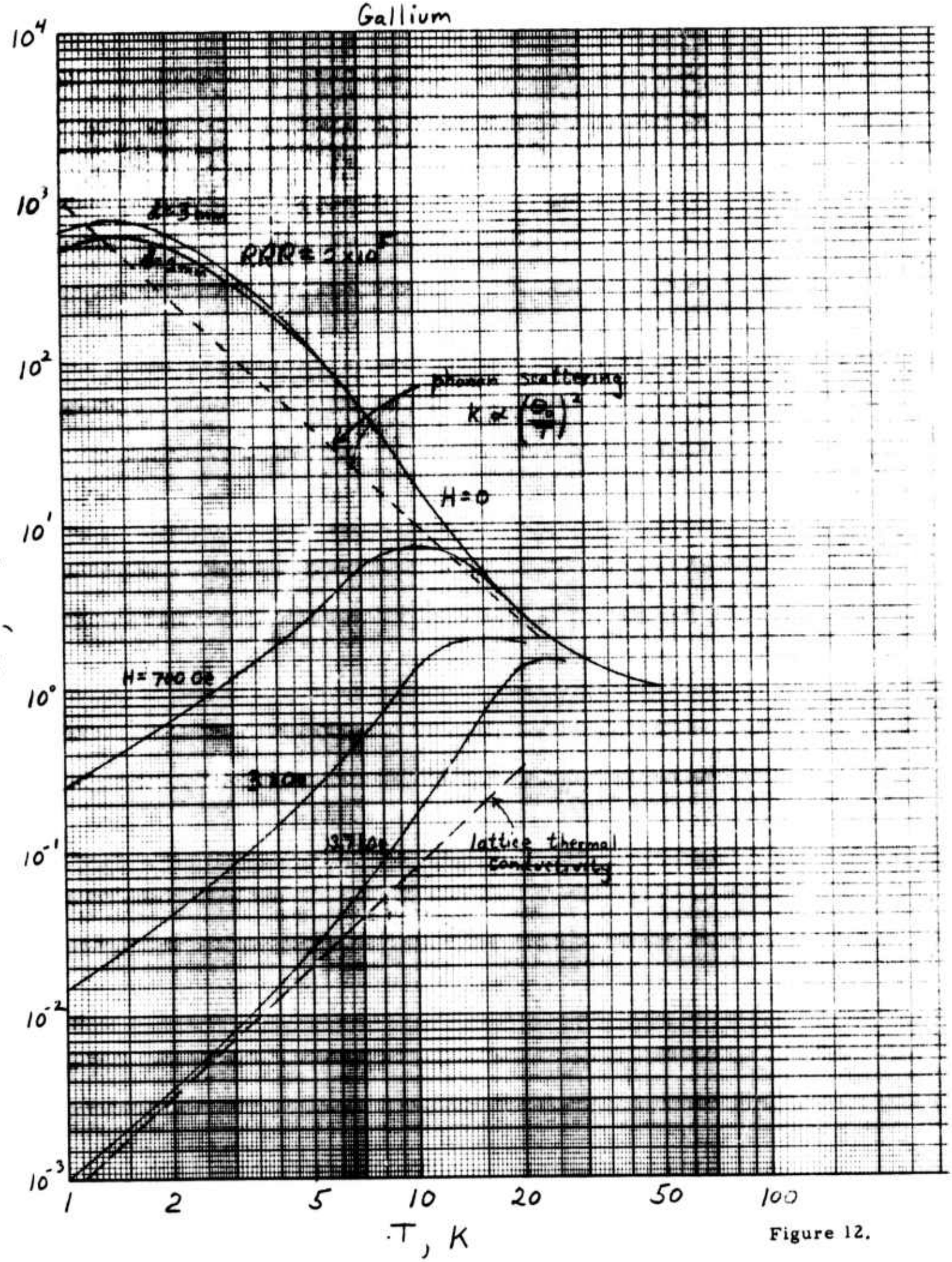
Gallium
RRR ≈ 2×10⁴
phonon scattering
k ∝ (Θ/T)²
H=0
H=740 Oe
lattice thermal conductivity
k, W/cm² K
T, K
10⁴
10³
10²
10¹
10⁰
10⁻¹
10⁻²
10⁻³
1
2
5
10
20
50
100

Figure 12.

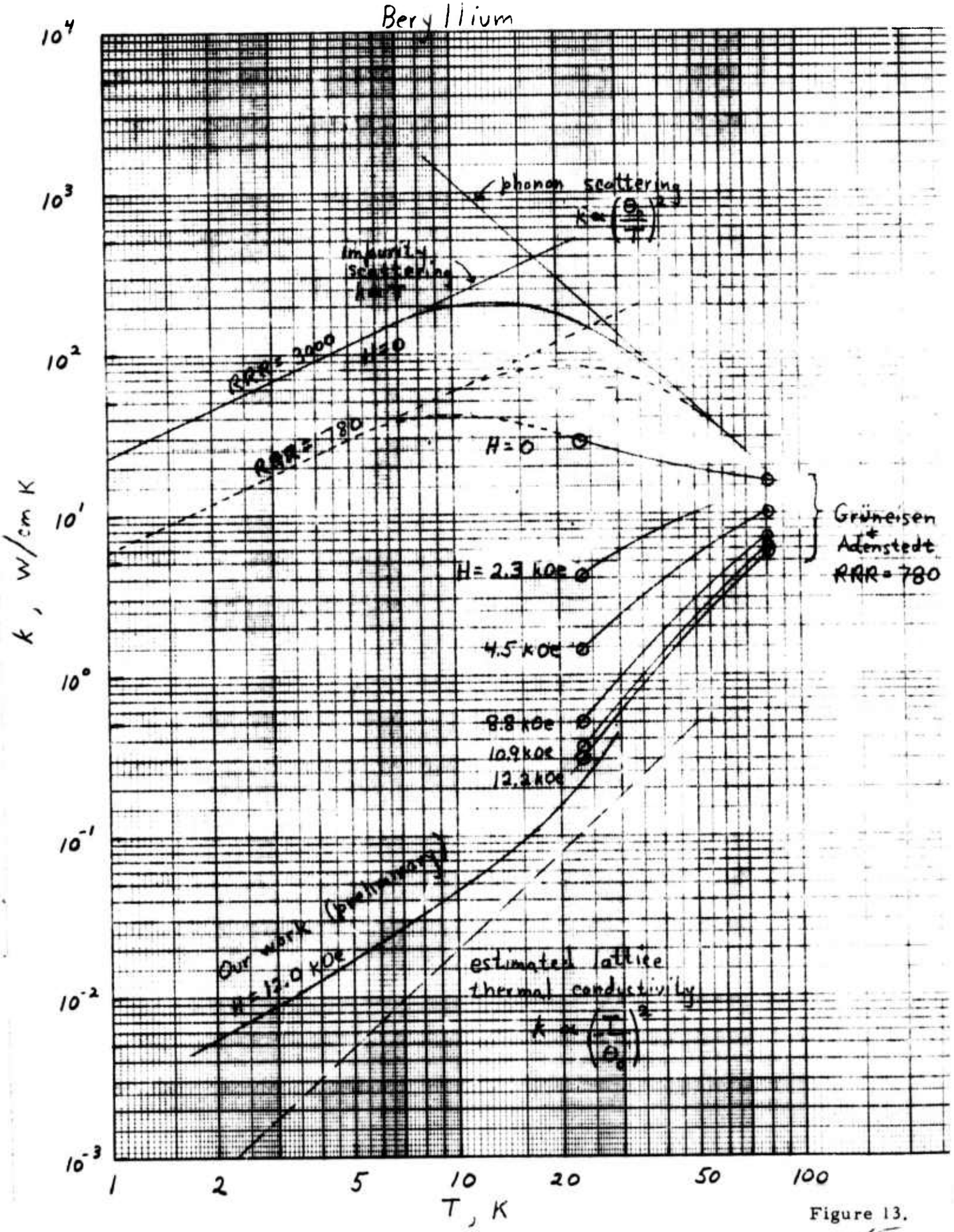
Beryllium
phonon scattering
$k \propto \left(\frac{\Theta_D}{T}\right)^3$
impurity scattering
RRR = 3000
H = 0
RRR = 780
H = 0
Grüneisen
Adenstedt
RRR = 780
H = 2.3 kOe
4.5 kOe
8.8 kOe
10.9 kOe
12.2 kOe
Our work (preliminary)
H = 12.0 kOe
estimated lattice
thermal conductivity
$k \propto \left(\frac{T}{\Theta_D}\right)^3$
k, W/cm K
T, K
10^4
10^3
10^2
10^1
10^0
10^{-1}
10^{-2}
10^{-3}
1
2
5
10
20
50
100

Figure 13.

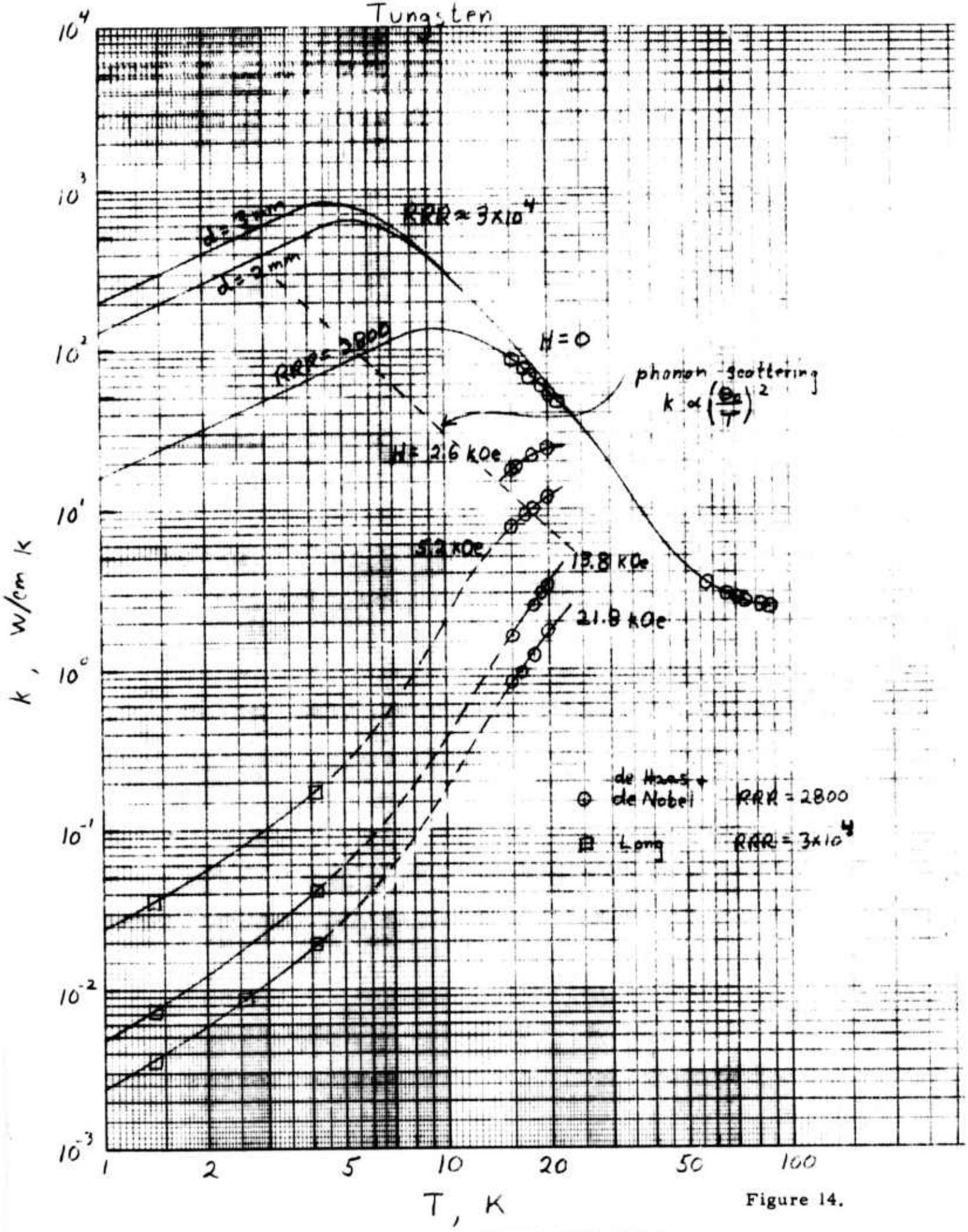
Tungsten
RRR ≈ 3×10⁴
d = 3 mm
d = 2 mm
RRR = 2800
H = 0
phonon scattering
k ∝ (Θ/T)²
H = 2.6 kOe
5.2 kOe
13.8 kOe
21.8 kOe
de Haas + de Nobel
RRR = 2800
Long
RRR = 3×10⁴
k, W/cm K
T, K
10⁴
10³
10²
10¹
10⁰
10⁻¹
10⁻²
10⁻³
1
2
5
10
20
50
100

Figure 14.

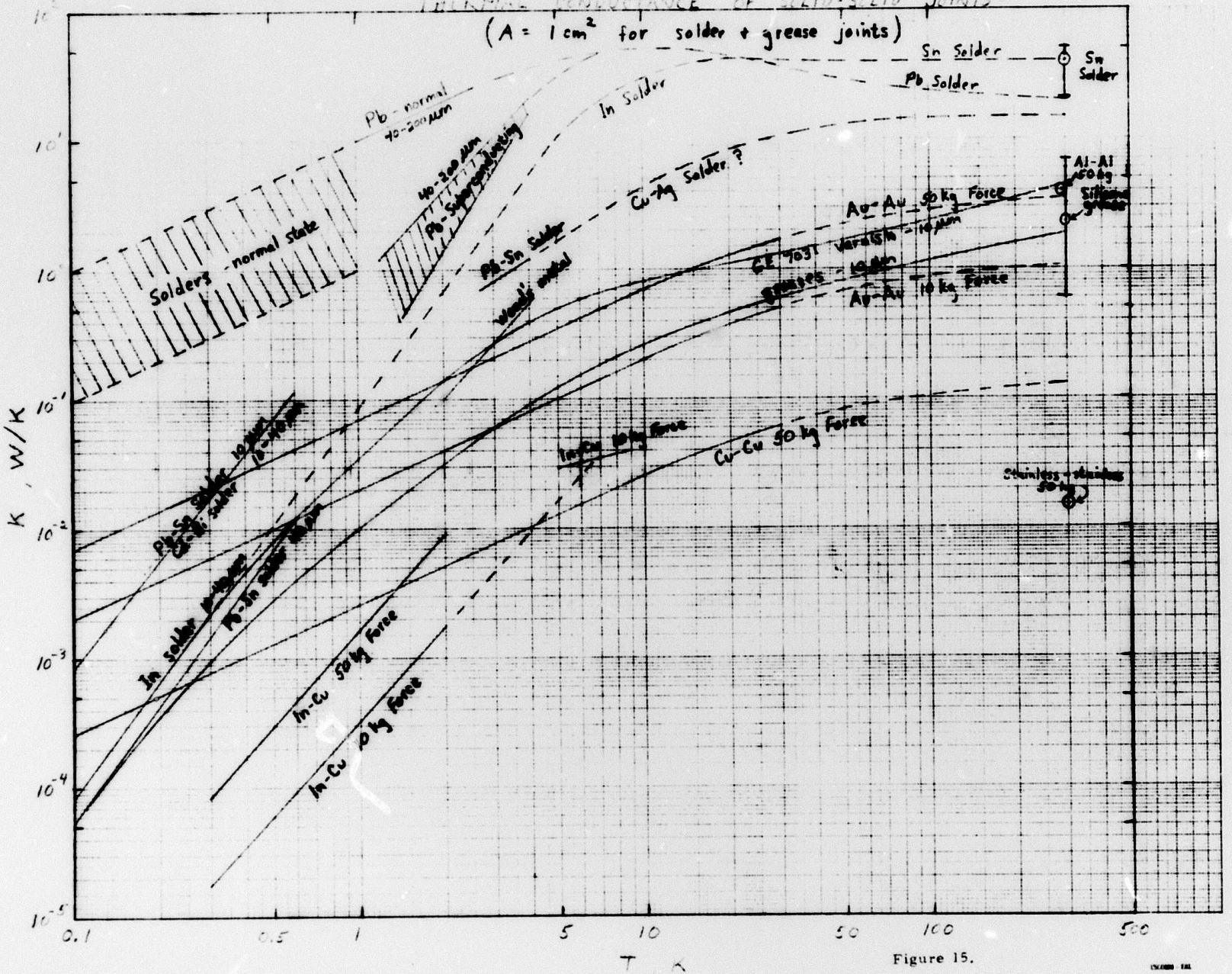
THERMAL CONDUCTANCE OF SOLID-SOLID JOINTS
(A = 1 cm² for solder + grease joints)
Sn Solder
Pb Solder
Sn Solder
In Solder
Pb - normal
40-200 μm
40-200 μm
Pb - Superconducting
Solders - normal state
Cu-Ag Solder ?
Al-Al 50 kg
Silicone grease
Au-Au 50 kg Force
GE 7031 varnish ~10 μm
stainless - stainless 10 kg
Pb-Sn Solder
Weak metal
Au-Au 10 kg Force
Pb-Sn Solder 10 kg
10-40 μm
Pb-Sn solder
Cu-Cu solder
In solder
Pb-In solder
In-Cu 50 kg Force
In-Cu 10 kg Force
Ta-Cu 10 kg Force
Cu-Cu 50 kg Force
Stainless - stainless 50 kg
K, W/K
T, K
0.1
0.5
1
5
10
50
100
500

Figure 15.